WHEAT YELLOW RUST IN URUGUAY: UNDERSTANDING THE GENETIC RESISTANCE IN A PANEL OF BREEDING AND COMMERCIAL GERMPLASM

Venancio Riella[1,2*], Bettina Lado[2], Federico Condón[1], Clara Pritsch[2], Martín Quincke[13], Monika Kavanová[1], Richard García[1], Fernando Pereira[1], Noelia Perez[1], Ariel Castro[2], Lucía Gutiérrez[3], Silvia Germán[1], Paula Silva[1]

[1] Instituto Nacional de Investigación Agropecuaria (INIA). Sistema Agrícola-Ganadero. Estación Experimental La Estanzuela. Ruta 50, km 11, 70006 Colonia, Uruguay

[2] Facultad de Agronomía, Universidad de la República, Garzón 780, 12900 Montevideo, Uruguay

[3] Department of Plant & Agroecosystems Sciences, University of Wisconsin-Madison, 1575 Linden Dr, Madison, Wisconsin 53705, USA

*Corresponding author: V. Riella; E-mail: vriella@fagro.edu.uy, Orcid-ID: https://orcid.org/0000-0001-5017-7857

Key message

Eight QTL conferring additive APR to YR were identified in wheat germplasm using GWAS. The high accuracy of GP models supports the feasibility of accelerating breeding for YR resistance.

Abstract

Wheat yellow rust (YR), caused by *Puccinia striiformis* f. sp. *tritici* (*Pst*), is among the most devastating diseases affecting wheat worldwide. Since 2000, YR has expanded into regions where it was previously not considered an economically important disease. The deployment of YR-resistant cultivars remains the most effective and sustainable control strategy. We assembled a diverse mapping panel (i) identify genomic regions associated with YR resistance using genome-wide association studies (GWAS), and (ii) assess the prediction accuracy of genomic prediction (GP) models for YR resistance. The panel of 366 wheat lines, including germplasm from INIA-Uruguay and other breeding programs, was phenotyped under artificial field inoculations in 2021 and 2022, and at the seedling stage using the same two *Pst* races used for field inoculations. GWAS identified eight genomic regions associated with field resistance, located on chromosomes 1B, 2B (three regions), 5B (two regions), 5D, 7B, explaining 4.9 to 21.2% of the phenotypic variability. None of these regions were identified with seedling resistance to race *Triticale2015b*, the most widely virulent race, indicating that they conferred adult-plant resistance. Moreover, these regions did not correspond to previously reported *Yr* genes. Two QTL on 2D and 3A were identified at the seedling stage to race *Triticale2015a* but did not contribute to field resistance. GP models achieved an average prediction ability of 0.64, highlighting their potential for

accelerating the selection of resistant lines. These findings provide valuable insights into the genetic basis of YR and offer robust tools for enhancing YR resistance breeding efforts in wheat.

Keywords

Puccinia striiformis, genome-wide association study (GWAS), quantitative disease resistance, genomic prediction (GP).

Abbreviations

A-BLUP: Additive best linear unbiased prediction
AIC: Akaike information criterion
APR: Adult-plant resistance
ASR: All-stage resistance
AUDPC: Area under the disease progress curve
BIC: Bayesian information criterion
BLUEs: Best linear unbiased estimators
bp: Base pair
CTAB: cetyltrimethylammonium bromide
DNA: Deoxyribonucleic acid
DS: Disease severity
FDR: False discovery rate
G-BLUP: Genomic best linear unbiased prediction
GBS: Genotyping-by-sequencing
GP: Genomic prediction
GWAS: Genome-wide association study
INIA: National Institute of Agricultural Research
KASP: Competitive allele-specific PCR
LD: Linkage disequilibrium
MAF: Minor allele frequency
MAS: Marker-assisted selection
MSE: Mean squared error
PCoA: Principal co-ordinate analysis
Pst: *Puccinia striiformis* f. sp. *tritici*
QTL: Quantitative trait loci
RGDP: Resistant Germplasm Development Program
RR-BLUP: Ridge regression best linear unbiased prediction
SNP: Single nucleotide polymorphism
WBP: Wheat breeding program

YR: Yellow rust

Introduction

Wheat (*Triticum aestivum* L.) ranks among the top three staple crops globally, alongside rice and maize, serving as a critical source of nutrition not only for its caloric contribution but also for its protein, vitamin, and fiber content, which are essential for human health (Bao and Malunga 2022). In recent years, global wheat production has been increasingly threatened by the emergence of new, more aggressive pathogen strains Hovmøller et al. 2008) adapted to diverse environments (Milus et al. 2006). Of particular concern is *Puccinia striiformis* Westend. f. sp. *tritici* (*Pst*), the causal agent of wheat yellow rust (YR) (Hovmøller et al. 2011; Sørensen et al. 2014). Historically, *Pst* has posed a significant challenge primarily in cooler climates; however, since 2000, the pathogen has shown increased aggressiveness (Hovmøller et al. 2008) and tolerance to higher temperatures, leading to its spread in regions previously considered too warm for its establishment (Wellings 2007; Milus et al. 2009). Additionally, distant geographic areas have reported YR epidemics, either as new incursions in previously unaffected regions or as re-emergences of novel, more widely virulent strains (Bahri et al., 2009; Hovmøller et al., 2023, Riella et al., 2024). As a result, YR has become one of the most severe and damaging diseases affecting common wheat globally, with potential yield losses reaching up to 100% under high disease pressure (Ali et al. 2014).

Genetic resistance to rust diseases is generally categorized into two types: all-stage resistance (ASR), also known as seedling resistance, which is expressed throughout the plant's lifecycle, and adult-plant resistance (APR) (Chen 2013). ASR is typically qualitative, conferred by one or a few major genes with largely dominant effects and follows a “gene-for-gene” relationship between host and pathogen (Flor 1955), in which each host gene provides resistance against pathogen races that carry the complementary avirulence gene. This type of resistance is race-specific, mediated by hypersensitive responses (Ayliffe et al. 2008), but generally provides short-lived effectiveness, as extensive use over large areas selects for new, virulent *Pst* races. Conversely, APR is effective in post-seedling stages, involves minor additive genes and confers partial resistance or “slow rusting” resistance, characterized by prolonged latent periods, fewer and smaller pustules, and reduced spore production (Singh et al. 2000, 2011; Bhavani et al. 2011). APR is generally race non-specific and considered durable; the accumulation of three to five minor APR genes can confer near-complete immunity (Singh et al. 2000). At least 87 YR resistance genes have been reported to date, but less than 30% confer APR (McIntosh 2024). The limited number of reported APR genes, coupled with their effects often being influenced by environmental factors and genetic background (Silva et al. 2015; Yuan et al. 2020; Liu et al. 2022), highlights the need to identify genomic regions associated with YR APR resistance in locally adapted materials. The discovery of new genomic regions is essential for making better use of the genetic diversity available and improving YR resistance effectivity and durability.

The identification of molecular markers associated with YR resistance is a promising approach to accelerate the development of resistant cultivars by identifying and pyramiding resistance genes within the same genotype. Among molecular markers, single nucleotide polymorphisms (SNPs) have gained widespread use due to their abundance across the genome and the significant reduction in genotyping costs in recent years (Crossa et al. 2017). One of the most utilized strategies for identifying the genetic basis of resistance to diseases is the genome-wide association study (GWAS). GWAS leverages linkage disequilibrium within a population to investigate associations between molecular markers and phenotypic traits. A statistically significant association suggests that the marker is linked to a genomic region contributing to the trait of interest, known as a quantitative trait locus (QTL) (Pritchard et al. 2000; Zhu and Yu 2009). GWAS has been successfully applied in wheat, identifying over 160 QTL across 49 regions on 21 chromosomes associated with YR resistance (Rosewarne et al. 2013; Maccaferri et al. 2015; Yuan et al. 2018). While GWAS enables fine-scale genome mapping using genetically diverse populations with extensive recombination histories, it also faces limitations, such as reduced power to detect rare allelic variants and the need to control for false positives, where marker-QTL associations are not due to physical linkage (Brachi et al. 2010; Wallace et al. 2014; Zuk et al. 2014). Moreover, the identification of QTL is often influenced by genotype-by-environment interactions, emphasizing the importance of detecting QTL that remain stable across different environments to ensure their utility in breeding programs (Gutiérrez et al. 2015).

Genomic prediction (GP) models using whole-genome data generally have higher power to capture small-effect loci compared to marker-assisted selection (MAS) (Heffner et al. 2009), particularly for complex traits controlled by many minor genes (Bernardo 2008; Mayor and Bernardo 2009; Lorenz et al. 2011; Cerrudo et al. 2018). GP leverages all genome-wide markers and phenotypic data to estimate genetic values and select candidates based on predicted genetic merit (Mrode 2014; Bernardo 2016; Crossa et al. 2017; Schmid and Bennewitz 2017). GP requires a training population that has been genotyped and phenotyped to calibrate a model, which can then predict genetic values of a selection population based solely on genotypic information (Bassi et al. 2016). GP is expected to reduce the time and cost required for cultivar development since annual genetic gains using GP are predicted to be two to three times higher than those achieved through conventional phenotypic selection due to shortened breeding cycles and increased selection accuracy (Jannink et al. 2010; Crossa et al. 2017). GP for disease resistance in crops has been applied in numerous studies (Poland and Rutkoski 2016), particularly for quantitatively inherited traits, with wheat rusts being among the most studied systems (Daetwyler et al. 2014; Rutkoski et al. 2014, 2015, 2016; Muleta et al. 2017; Ornella et al. 2017). GP in wheat rust resistance breeding could accelerate selection cycles and help pyramid APR genes (Rutkoski et al. 2011).

Objective

With the aim of contributing to the sustainability of wheat production through the development of YR resistant cultivars, this study focuses on two main objectives: (i) to identify genomic regions

associated with YR resistance in diverse wheat germplasm through GWAS, and (ii) to assess the prediction accuracy of GP models for YR resistance in wheat lines.

Materials and methods

Plant material

The GWAS and GP panel consisted of 366 diverse spring bread wheat genotypes, representing the most currently and historically important wheat cultivars and advanced breeding lines of Uruguay. The panel includes lines of different origin: 172 lines from the INIA Resistant Germplasm Development Program (INIA-RGDP), developed to introgress APR to leaf rust, primarily from CIMMYT germplasm, and to address other prevalent diseases in Uruguay prior to 2017, 117 lines from the INIA-Wheat Breeding program (INIA-WBP), including advanced and elite lines as well as released varieties, representing a century of wheat breeding in the country, 73 cultivars from other breeding programs sown in Uruguay, and four check lines, selected for their diversity in maturity date and susceptibility to YR (**Table S1**). For most of the lines present in the panel there was not previous YR phenotypic information since the disease was not present prior to 2017. Cultivar Morocco was used as a susceptible check in field and seedling trials but was not included in the GWAS and GP panel.

Phenotypic trait evaluation

Field yellow rust and heading date phenotyping

Field experiments were conducted at INIA La Estanzuela Experimental Station, (latitude 34.3°S, longitude 57.7°W, elevation 70 masl), Colonia, Uruguay, during two consecutive crop seasons (2021 and 2022). Sowing dates were May 14th 2021 and May 4th 2022. The experimental design consisted of an alpha lattice resolvable incomplete block design with three replications. Plots consisted of single 1 m long rows 0.30 m apart. Spreader rows of a mixture of susceptible cultivars (Morocco, Avocet S, Fuste, Algarrobo, Ceibo, and Onix) were sown perpendicular to all plots to ensure the presence and even distribution of the disease. Artificial inoculations were performed on the spreader rows with a mixture of the two most prevalent races in previous years (*Triticale2015a* and *b*), both races belonging to the *PstS13* genetic group (Riella et al. 2024). Three and six inoculations with a suspension of inoculum in lightweight mineral oil Soltrol 170 (Phillips Petroleum Co., Borger, TX) were performed in 2021 and 2022 respectively, between July 20 and August 20. In 2021 the experiment was rainfed, meanwhile, in 2022, due to dry weather conditions, the trial was irrigated using a sprinkler system. Days to heading for each plot were calculated as the days from seedling emergence to heading date. Heading date was recorded based on the crop ontology trait CO_321:0000840 as the date when 50% of the head emerged in 50% of the plot (https://cropontology.org).

First disease assessment took place when the susceptible check Morocco displayed a disease severity (DS) of at least 50% and continued for six times at 7-12 days intervals. For each evaluation, DS was visually scored as the percentage of infected tissue (0 – 100%). . The six DS obtained for each plot

were combined in a single value as the area under the disease progress curve (AUDPC) according to following formula:

$$AUDPC = \sum_{i=1}^{N_i-1} \frac{(y_i + y_{i+1})}{2}(t_{i+1} - t_i)$$

where AUDPC for each plot is given by y_i rust DS at the time of recording t_i, y_{i+1} rust infection rate at the time of recording t_{i+1}, N the number of records to assess the DS from 1 to 6.

Statistical analyses for field yellow rust phenotyping

The phenotypic data were analyzed using R software (R Core Team 2024). To evaluate quality of each trial and accurately estimate the phenotypic means, the AUDPC data was analyzed independently for each year (2021 and 2022) fitting a linear mixed model with the lme function of the lme4 package (Bates et al. 2015). The statical model, followed the experimental design and including days to heading as a covariate, was:

$$y_{ijk} = \mu + \tau_i + \beta_j + \gamma_{k(j)} + \lambda(x_{ijk} - \bar{x}) + \varepsilon_{ijk} \quad \textbf{[1]}$$

where y_{ijk} represents the AUDPC (response variable) measured on the i-th wheat line in the j-th complete replicate, in the k-th incomplete block, μ the overall mean, τ_i the relative effect of the i-th wheat line, β_j the effect of the j-th complete replicate, and $\gamma_{k(j)}$ the random effect of the k-th block nested in the j-th complete replicate which is assumed to be random with normal distribution centered on zero and with constant variance (σ_γ^2), $\lambda(x_{ijk} - \bar{x})$ is a covariate term for days to heading correction, where x_{ijk} is days to heading, $\bar{x}$ the mean for days to heading, and λ the regression coefficient associated with the covariate. Given that the panel consists of highly diverse lines with important variability in maturity, days to heading was included as a covariate in the model. This adjustment aimed to minimize potential noise that could lead to the identification of regions associated with phenology rather than YR resistance. This model assumes that the errors (ε_{ijk}) are independent random variables, normally distributed with zero mean and constant variance (σ_ε^2), and that there is no interaction between blocks and treatments (Di Rienzo et al. 2009).

To select the best model for estimating phenotypic means while incorporating information from the experimental design, spatial effects, and covariate (days to heading), the fit of the baseline model (model **[1]**) was compared to alternative models. These alternatives included models that incorporated the spatial position of the plot in the field as an additional factor (e.g., column effects). They also considered models that assumed different variance-covariance structures for the experimental errors, such as Gaussian, spherical, and exponential models, to account for potential correlations among the experimental units. Model comparisons were conducted separately for each year using fit criteria such

as the Akaike Information Criterion (AIC) and Bayesian Information Criterion (BIC), as well as performance indicators, including the correlation between observed and predicted values and broad-sense heritability (H^2) estimates. Broad-sense heritability was calculated for each trial, the variance components (σ_g^2 genotypic variance and σ_{error}^2 error variance) were estimated from equations **[1]** and **[2]** with genotypes as random effects, using equation $H^2 = \sigma_g^2/(\sigma_g^2 + \sigma_{error}^2/rep)$. The error variance was corrected for the number of replicates (Falconer and Mackay 1996). Due to the strong correlation between environments and similar accuracy between the best models each year, the adjusted means (Best Linear Unbiased Estimators, BLUEs) for AUDPC for each genotype were obtained and estimated by fitting a combined model using data from both years. This model is similar to model **[1]** except that it includes the year effect (α_l) as follow:

$$y_{ijkl} = \mu + \tau_i + \alpha_l + \beta_{j(l)} + \gamma_{k(jl)} + \lambda(x_{ijkl} - \bar{x}) + \varepsilon_{ijkl} \qquad \textbf{[2]}$$

Seedling yellow rust phenotyping

Greenhouse trials were conducted to determine resistance at the seedling stage of the panel, which indicates the presence of ASR genes. The phenotyping was conducted during 2023 at INIA La Estanzuela Experimental Station, using two *Pst* races used in field inoculations, *Triticale2015a* and *Triticale2015b* (Riella et al. 2024). Eight seeds of each genotype were sown in plastic trays with substrate (mixture of one third soil, one third vermiculite and one third seedbed substrate: Potting mix, Bioterra), 25 genotypes per tray, plus Morocco as the susceptible check. Fully expanded leaves (8–10 days after sowing) were inoculated by spraying urediniospores suspended in Soltrol 170, incubated at 10ºC in a dew chamber overnight and then kept in the greenhouse at 15–25 °C with supplemental lighting. Infection type (IT) was recorded for each genotype 15–20 days after inoculation based on a 0–9 scale (McNeal et al. 1971) (crop ontology CO_321:0000606), lines with IT values of 0-3 were considered resistant, 4-6 intermediate and 7-9 susceptible. Two complete replicates were used for each genotype and race. The IT adjusted means for each genotype were obtained by fitting a linear model with the lm function in software (R Core Team 2024). The statistical model used was $y_{ij} = \mu_i + \varepsilon_{ij}$ where y_{ij} represents the IT value (response variable) measured on the i-th wheat line in the j-th replicate, μ the overall mean, this model assumes that the errors (ε_{ij}) are independent random variables, normally distributed with zero mean and constant variance (σ_ε^2).. For each inoculation, a tray with the set of YR differential lines was included in order to corroborate the identity and purity of the race used.

Genotypic Data

The genomic DNA of the 366 wheat lines was isolated from fresh leaves of 20-day old plants by the CTAB method (Saghai-Maroof et al. 1984). Genotyping was performed by Genotyping-by-sequencing (GBS) using an Illumina 150 bp paired-end sequencer at the University of Wisconsin-Madison DNA Sequencing Facility. Analysis of the genotypic data first involved SNP calling using the

TASSEL GBSv2 pipeline (Glaubitz et al. 2014), and the cv Chinese Spring as the reference genome (IWGSC CS RefSeq v2.1) (Zhu et al. 2021). SNPs with >80% missing data and SNPs with a minor allele frequency (MAF) less than 0.01 were also removed. Missing data were imputed with BEAGLE 5.4 (Browning et al. 2018). Data were transformed to numerical coding (0, 1, and 2 for homozygotes for the major allele, heterozygotes, and homozygotes for the minor allele, respectively) for analyses, obtaining the complete matrix with a total of 156,032 SNPs.

In addition, the presence of APR genes *Yr18* (*TCCIND*, Rasheed et al. 2016), *Yr29* (*SNP1G22,* Lagudah et al., pers. comm.), and *Yr46* (*csSNP856,* Forrest et al. 2014) within the wheat panel was verified based on competitive allele-specific PCR (KASP) assays. These assays were performed at INIA-Las Brujas lab following CIMMYT protocols (Dreisigacker et al. 2016).

Population structure and Linkage disequilibrium (LD)

The genetic structure of the population was studied using the Admixture program (Alexander et al. 2009) to determine the number of subpopulations (K). The ΔK was observed as the number of subpopulations increased (K = 0 to K = 20). Additionally, with the SNP matrix obtained in the previous step, Euclidean genetic distances were calculated between the panel lines, from which a principal co-ordinate analysis (PCoA) and a genetic distance plot were created using the R package ade4 (Dray and Dufour 2007). The extent of linkage disequilibrium (LD) in this association panel was calculated according to (Zhang et al. 2018), based on pairwise squared LD correlation coefficients (r^2) for all intrachromosomal SNP loci. Nonlinear model, described by Remington et al. (2001), was fitted to study the relation between r^2 and physical distances. To fit the non-linear model nls function in R was used (R Core Team 2024). The physical distance at which LD fell below the r^2 thresholds determined according to Zhang et al. (2018)Haga clic o pulse aquí para escribir texto. was used to define the confidence intervals of the QTL detected in the GWAS analysis.

Genome-wide association analysis between phenotype and genotype

GWAS was performed to identify genomic regions associated with YR resistance, using a matrix of 156,032 SNPs and 366 genotypes. The R package GWASpoly (Rosyara et al. 2016) was used to conduct the GWAS. GWAS was performed using mixed model with best linear unbiased estimates (BLUE) for AUDPC (from join analysis of both years) as response variable, SNP coded as 0,1,2 as fixed effect and random polygenic effect to control for population structure, commonly known as the K model (Yu et al. 2006). This method uses a covariance matrix, effectively treating all markers as random effects. However, as this can lead to "proximal contamination" (Listgarten et al. 2012), where markers tested as fixed effects are also included as random effects, reducing model performance. The leave-one-chromosome-out (LOCO) approach (Yang et al. 2014) was used to improve accuracy by calculating covariance matrices for each chromosome using markers from other chromosomes. The results were summarized with Manhattan plots to visualize associations between SNPs and traits, utilizing functions

in GWASpoly. Population structure was controlled by incorporating a kinship matrix, as implemented in GWASpoly, to avoid spurious associations. Quantile–quantile (QQ) plots were used as a visual criterion for assessing the model fit of the GWAS. To minimize the risk of false positives, GWASpoly applies corrections such as the false discovery rate (FDR). In this study, a significance threshold of FDR=0.1 was used.

QTL identified in this study were named following (Boden et al. 2023), using the prefix "Q" for QTL, "Yr" for yellow rust, and "uy" to indicate Uruguay, followed by a hyphen and the corresponding chromosome number and genome and the chromosome arm (short: S, long: L). When more than one QTL were identified on the same chromosome arm, an additional number was added after a decimal point (Boden et al. 2023). Additionally, the chromosome arm (short: S, long: L) was also specified.

A region was considered a QTL if it contained at least two markers in LD above the threshold. All significantly associated markers within each region were considered to define haplotypes. The physical position of the first and last markers above the threshold was defined as the start and end of the QTL, respectively. The p-value, effect, and percentage of explained variance for each QTL were obtained by fitting a separate linear regression model for each QTL. The regression model includes BLUE of AUDPC as the response variable. It is regressed on a dichotomous variable where one (1) was assigned to the favorable more resistant haplotype (lower AUDPC) and two (2) to the more susceptible haplotype (higher AUDPC).

To determine whether the significant SNPs detected in this study were located in the same position as previously reported *Yr* genes and resistance QTL, the physical locations of the identified genomic regions were compared with positional data from the most updated database of wheat rust resistance genes and QTL currently available in the literature (McIntosh 2024; Tong et al. 2024).

To determine the effect of accumulation of favorable YR QTL alleles on AUDPC, wheat lines were grouped according to their number of favorable QTL alleles. The AUDPC means for each group were compared using a Tukey multiple comparisons test ($P < 0.05$).

Genomic prediction (GP)

We assessed the predictive ability of seven genomic prediction models with different assumptions regarding marker effect distributions. The first model, additive best linear unbiased predictor (A-BLUP), used only the pedigree-based relationship matrix without including genetic marker data. The pedigree matrix was created using the prepPed and makeA functions of the nadiv package (Wolak 2012) based on parental information from INIA-WBP, however, information was missing for 44 of the commercial lines present in the panel (12% of the total). Subsequently, other models incorporating genetic information in different ways and assuming different marker effect distributions were tested. The models compared included two mixed models: ridge-regression best linear unbiased predictor (RR-BLUP), which uses information from all markers, genomic best linear unbiased predictor (G-BLUP),

which leverages genetic distance between lines for predictions, and four types of Bayesian models: Bayesian A (BA), Bayesian B (BB), Bayesian C (BC), and Bayesian Lasso (BL).

To conduct the comparisons, a 10-fold cross-validation with 100 iterations was performed. This validation strategy involves randomly dividing the panel lines (366 lines) into 10 groups (with 36 or 37 lines); nine groups were used to train the model, and predictions were made for the lines in the tenth group. This process was repeated for each of the 10 groups over 100 iterations. All analyses were conducted in R software, using the BGLR package (Pérez and De Los Campos 2014).

Predictive ability was estimated as the Pearson's correlation between observed and predicted values in each iteration. The mean squared error (MSE) was calculated as the difference between observed and predicted values. Additionally, in a second phase, identified QTL from the previous GWAS were sequentially added to the genomic prediction model as fixed effects, ordered by the amount of variance they explained. The performance of these models was then compared with the model excluding these fixed effects.

Results

Phenotypic Traits

Field trials in both years had uniform infection levels, with high infection levels in check lines. The AUDPC values for the check cultivar Morocco in 2021 ranged between 5075 and 5260 among reps, and in 2022, between 6125 and 6475. The panel of 366 wheat lines displayed a continuous distribution of YR AUDPC values over the two years (**Fig. S1**), ranging from 0 to 5491 (**Table 1**). The average AUDPC for INIA-RGDP lines was the lowest with value of 2624 followed by the cultivars from other breeding programs with 2908, while INIA-WBP lines presented an average AUDPC of 3433. The proportion of phenotypic variance attributed to genetic factors, as estimated by broad-sense heritability (H^2) was 0.98 (**Table S2**). Seedling tests also showed high and uniform infection, with the check cultivar Morocco consistently exhibiting IT scores of 8 or 9. In seedling tests with race *Triticale2015a*, 30.6% of genotypes showed resistant reactions (IT = 0–3), 42.6% displayed intermediate reactions (IT = 4–6), and 26.8% were susceptible (IT = 7–9). For the more widely virulent race *Triticale2015b*, 18.3% of genotypes were resistant, 41% showed intermediate reactions, and 40.7% were susceptible (**Fig. S2**).

Table 1. Average (Mean), minimum (Min), maximum (Max), and standard deviation (SD) and heritability (H^2) of field yellow rust area under the disease progress curve (AUDPC) and seedling infection type (IT) of the 366 wheat lines of the genome-wide association study (GWAS) panel evaluated in field conditions during 2021-2022, and under greenhouse conditions in the seedling stage after inoculation with two locally prevalent *Pts* races.

Resistance type	Trait	Trial	Mean	Min	Max	SD	H^2
Field evaluation	AUDPC	2021	2949	0	4973	1293	0.98

		2022	3234	0	6468	1793	0.98
		Both years	2955	0	5491	1423	0.92
Seedling stage	IT	Triticale2015a	4.24	0	9	2.18	0.95
		Triticale2015b	5.17	0	9	2.08	0.98

The BLUEs for YR AUDPC values obtained from field trials were calculated for each year using the best-fitting statistical model. In addition, all models evaluated showed similar accuracy and fit indicators (AIC, BIC, heritability and correlation between observed and predicted values). For 2021, the model base was selected, as it showed lower AIC and BIC values, minimal differences in heritability and correlation between observed and predicted values compared to the same model but including the column effect (**Table S2**), and a homogeneous and normal residual distribution (**Fig. S3**). In contrast, for 2022, the model including the random column effect provided a better fit, evidenced by lower AIC and BIC values, higher heritability and correlation between observed and predicted values (**Table S2**), and a more uniform residual distribution (**Fig. S3**). In both years, incorporating a spatial correlation structure for the residuals did not improve model fit (**Table S2**).

Pearson correlation analysis of the AUDPC BLUEs from the selected models for 2021 and 2022 revealed a strong correlation between the two years (r = 0.74), and similarly high correlations among replicates within each year (**Fig. S1**). Based on these results, the data from both years were combined into a single dataset and AUDPC BLUEs were obtained using the model **[2]** which includes effects for experimental design, days to heading as covariate and the year effect for the combined data from 2021 and 2022 (**Table S2**).

Genotypic Data

SNP calling using TASSEL identified 237,282 SNPs for all lines. SNPs with >80% missing data (~38,000) and those with a minor allele frequency (MAF) <0.01 (~43,000) were removed. The final dataset included 366 wheat lines and 156,034 SNPs, with missing data imputed using BEAGLE. The detected SNPs provided good coverage of all chromosomes, with a low marker saturation in the D genome (**Fig. S4**). Heatmap with cluster analysis using the Euclidean distance matrix revealed no distinct groups (**Fig. S5 A**). Similarly, no clear clustering was observed in the PCoA, where the two principal components explained only 0.020 and 0.022 of the variances, respectively, with no relationship to YR AUDPC values or the panel lines' origins (**Fig. S5 B and C**). The admixture analysis also provided no significant evidence of population stratification (**Fig. S5 D**). Together, these results indicated that including subpopulation effects was unnecessary for subsequent analyses. Linkage disequilibrium (LD) analysis showed rapid LD decay along the chromosomes, with average r^2 values falling below 0.2 within 0.12 Mb.

Genome-Wide Association Study (GWAS)

Eight genomic regions associated with field YR resistance were identified (**Fig. 1**) using a false discovery rate (FDR) threshold of $-\log_{10}(p)$, $P < 0.1$ resulting in a value of 3.7. These regions were located on chromosomes 1BL, 2BL (three regions), 5B (one in 5BS and the other in 5BL), 5DL and 7BL (**Table 2**). The three regions identified on chromosome 2BL (as well as the two on chromosome 5B) were considered independent because their physical distance was larger than the 0.12 Mb distance estimated by the LD analysis. Regions with at least two markers above the significance threshold were classified as quantitative trait loci (QTL). When we analyzed all significantly associated markers within each QTL region together to define haplotypes, we found only two haplotypes in each QTL region.

The QTL explaining the highest proportion of the phenotypic variance was *QYr.uy-2BL.3* (21.24%), followed by *Qyr.uy-2BL.2* (12.1%), *Qyr.uy-5BS*, *Qyr.uy-5BL*, *Qyr.uyt-5DL*, *Qyr.uyt-7DL, Qyr.uyt-2BL.1* and *Qyr.uy-1BL* explained progressively lower proportions of the phenotypic variance (**Table 2**). The effect of each QTL on AUDPC is illustrated by the boxplots in **Fig. 2**. The favorable QTL allele (associated with lower AUDPC values) was assigned the value "1", while the less favorable QTL was assigned the value “2”. Furthermore, **Fig. 2** represents the distribution of the number of lines according to their YR AUDPC values for each allele of each QTL, based on the width of the surface surrounding each boxplot.

The proportion of lines carrying the favorable YR resistant QTL varied according to their origin (INIA-WBP, INIA-RGDP, and cultivars from other breeding programs). *Qyr.uy-5BL* was present in 84% of all lines, *Qyr.uy-1BL* in 80%, *Qyr.uy-5DL* in 75%, *Qyr.uy-7BL* in 61%, *Qyr.uy-5BS* in 36%, *Qyr.uy-2BL.1* in 35%, *Qyr.uy-2BL.3* in 27%, and *Qyr.uy-2BL.2* in 18%of the lines. *Qyr.uy-1BL*, *Qyr.uy-2BL.3*, *Qyr.uy-5BS*, *Qyr.uy-5BL*, and *Qyr.uy-7BL* were found in a higher percentage of lines from INIA-RGDP, in contrast, *Qyr.uy-2BL.1* and *Qyr.uy-2BL.2* were more frequent in cultivars from other breeding programs (**Table 3**).

Figure 1. Manhattan plot for yellow rust (YR) resistance based on area under the disease progress curve (AUDPC) values from 2021 and 2022 field trials combined in 366 wheat lines of the panel. The horizontal line indicating the genome-wide significance threshold

Table 2. Summary of significant Quantitative trait loci (QTL) associated with yellow rust (YR) resistance. The table includes QTL identified for field resistance based on area under the disease progress curve (AUDPC) combined values from 2021 and 2022, and seedling resistance based on infection types (IT) for *Pst* race *Triticale2015a* of 366 wheat lines of the panel.

Trait	QTL	Chr.[a]	Physical position of flanking markers (Mb)[b]	P value	Effect	PVE (%)[c]

Field AUDPC	*Qyr.uy-1BL*	1B	540.16 - 541.70	$2.7e^{-5}$	-848.82	4.9
	QYr.uy-2BL.1	2B	400.34 - 464.32	$5.5e^{-6}$	-706.7	5.7
	QYr.uy-2BL.2	2B	564.47 – 564.82	$9.1e^{-12}$	-1268.2	12.1
	QYr.uy-2BL.3	2B	690.94 – 709.24	$<2e^{-16}$	-1425.2	21.2
	QYr.uy-5BS	5B	69.74 – 74.92	$3.5e^{-10}$	-973.2	10.6
	QYr.uy-5BL	5B	537.95 – 538.48	$1.3e^{-8}$	-1156.8	8.6
	QYr.uy-5DL	5D	548.10 – 552.03	$2.1e^{-7}$	-898.4	7.3
	QYr.uy-7BL	7B	617.83 – 657.05	$1.5e^{-6}$	-777.2	6.6
Seedling IT *Triticale2015a*	*QYr.uy-2DS*	2D	15.34 - 18.30	$2.2e^{-16}$	-2.3	19.1
	QYr.uy-3AL	3A	488.45 - 490.15	$5.4e^{-8}$	-1.4	7.9

[a]Chromosome, [b]Physical positions (Mb) of flanking markers are based on the Chinese Spring reference IWGSC RefSeq v1.0; [b]PVE, phenotypic variance explained.**Figure 2.** The effects of quantitative trait loci (QTL) identified for yellow rust (YR) resistance based on area under the disease progress curve (AUDPC) combined values from the 2021 and 2022 field trials. The AUDPC value for the 366 wheat lines of the GWAS panel are shown based on their haplotype for each QTL, with (1) being the more favorable resistant allele, and (2) being the more susceptible allele.

Table 3. Percentage of lines carrying the favorable allele for each quantitative trait loci (QTL) associated with area under the disease progress curve (AUDPC) in field trials and infection type (IT) in seedling tests for the *Triticale2015a* race, within each group of lines according to their origin and the full panel of 366 wheat lines.

Trait	QTL	Line origin			Full panel
		INIA-RGDP	INIA-WBP	Other breeding programs	
Field AUDPC	*QYr.uy-1BL*	84	80	68	80
	QYr.uy-2BL.1	19	33	77	35
	QYr.uy-2BL.2	14	12	38	18
	QYr.uy-2BL.3	30	21	27	27
	QYr.uy-5BS	44	23	38	36
	QYr.uy-5BL	89	82	77	84
	QYr.uy-5DL	78	80	62	75
	QYr.uy-7BL	67	54	62	61
Seedling IT *Triticale2015a*	*QYr.uy-2DS*	20	25	14	20
	QYr.uy-3AL	25	26	32	27

The lines were grouped into six categories based on the number of favorable QTL alleles for YR AUDPC determined in the field trials, ranging from zero to eight favorable QTL. A pronounced in AUDPC values was observed as the number of favorable QTL increased (**Fig. 3**).

Figure 3. Effect of the number of quantitative trait loci (QTL) associated with yellow rust (YR) resistance based on area under the disease progress curve (AUDPC) combined values from 2021 and 2022 field trials of 366 wheat lines. The number of lines in each group according to their origin is indicated below each boxplot. Different letters above the boxplots indicate significant differences ($P < 0.05$) in AUDPC between groups, as determined by Tukey′s test. Boxplots show the distribution of a dataset through five key summary statistics: minimum (lower whisker), first quartile (bottom of the box), median (line inside the box), third quartile (top of the box), and maximum (upper whisker). Points beyond the whiskers are values outside 1.5 times the interquartile range from the quartiles.

Two genomic regions associated with YR seedling resistance to race *Triticale2015a* were identified (**Fig. S6 A**). Haplotype analysis revealed two haplotypes for each identified region. The QTL on chromosome 2D explained 19.1% of the phenotypic variance, while another QTL on chromosome 3A accounted for 7.9% (**Table 2**). The favorable allele for *QYr.uy-2DS* was present in 20% of all lines, while the favorable allele for *QYr.uy-3AL* was found in 27%. The favorable allele of *QYr.uy-3AL* was present in a higher proportion in INIA-WBP lines while the favorable allele of *QYr.uy-2DS* was present in a higher proportion of cultivars from other breeding programs (**Table 3**). GWAS for the more widely virulent race *Triticale2015b* did not identify any genomic regions significantly associated with YR resistance (**Fig. S6 B**).

Through GWAS, we detected one mayor QTL for days to heading on chromosome 2D, which did not co-localized with any of the QTL associated with YR resistance in the field or seedling trials (**Fig. S6 C**). Additionally, the identified QTL for YR resistance did not coincide with the location of previously reported phenology-related genes (data not shown).

Genomic Prediction (GP)

From the seven GP models evaluated, the A-BLUP model had the lowest prediction accuracy, with correlations between observed and predicted AUDPC values below 0.5, and the highest MSE (**Fig. S7 A**). The G-BLUP and RR-BLUP models performed similarly, achieving correlations between observed and predicted AUDPC values around 0.7 and a lower MSE compared to other models MSE (**Fig. S7 B**). Bayesian models (BA, BB, and BC) demonstrated comparable prediction accuracies as G-BLUP and RR-BLUP, with correlations near 0.7 and moderate MSE values. In contrast, the Bayesian LASSO (BL) model exhibited poorer performance, with accuracy closer to the A-BLUP model and higher MSE values. Overall, G-BLUP, RR-BLUP, and Bayesian (BA, BB and BC) models showed the most robust predictive performance.

The BL model performed worse than RR-BLUP, and the prediction ability of RR-BLUP model was nearly identical to that of the G-BLUP model. Therefore, the G-BLUP model was selected for further comparisons due to its simplicity and lower computational requirements. Subsequently, we investigated whether incorporating fixed effects for the identified QTL could improve the GP accuracy. We compared the AUDPC predictions from the G-BLUP model without fixed QTL effects and with the sequential addition of fixed effects for the eight QTL, added in descending order of the explained variance. The inclusion of fixed effects in the model led to an improvement in prediction accuracy, with correlations between observed and predicted values increasing from an average of 0.64 in the G-BLUP model without fixed effects to 0.69 in models that included GWAS-identified QTL as fixed effects. Notably, the inclusion of *QYr.uy-2BL.3* alone was sufficient to achieve this improvement, as no further gains were observed when additional QTL were incorporated as fixed effects (**Fig. S8 A**). Moreover, the inclusion of fixed effects also impacted the MSE, which was reduced by 10.4% when *QYr.uy-2BL.3* was included, compared to the G-BLUP model without it (**Fig. S8 B**).

Discussion

Recent outbreaks of YR in major wheat-producing regions worldwide (Bouvet et al. 2022) pose a significant threat to wheat production and global food security. Particularly in the Southern Cone of South America, recent epidemics (Campos et al. 2016; Germán et al. 2018; Campos 2020; Silva et al. 2023; Riella et al. 2024) have been linked to the incursion of new *Pst* genetic groups and races characterized by increased aggressiveness and improved adaptation to diverse temperature ranges (Rajaram and Campos 1974). Argentina and Uruguay are located in the same rust epidemiological zone (Rajaram and Campos 1974) where there are no geographical barriers for urediniospores dispersal, which likely explains the almost simultaneous development of severe epidemics in both countries (Rudolf and Job 1931). In Uruguay, *Pst* was first detected in 1929 (Rudolf and Job 1931). It caused widespread epidemics and substantial yield losses across the Southern Cone region during 1929 and 1930 (Boerger 1934; Vallega 1938). From its initial detection until 2016, *Pst* outbreaks remained sporadic, rarely reaching epidemic levels in Uruguay (Germán and Caffarel 1999; Germán et al. 2007, 2018). However, since 2017, wheat crops grown in Uruguay and Argentina have experienced widespread epidemics, likely due to an earlier onset of the disease during the growing season, the extensive planting of susceptible or moderately susceptible cultivars (covering more than 50% of the wheat-growing area) (Silva et al. 2023), and the emergence of novel races in the region (Riella et al. 2024).

YR is currently the wheat foliar disease, which requires the largest number of fungicide applications in Uruguay. Deploying resistant wheat cultivars is an economically and environmentally sustainable strategy, significantly reducing the use of fungicides (Chen 2005, 2013). Therefore, it is essential to identify diverse resistance sources effective under local conditions, which can be utilized in

breeding programs to introgress and pyramid resistance genes into locally adapted germplasm. From the perspective of resistance breeding, the most relevant phenotype is that expressed in the field (APR). However, this must be complemented with the seedling phenotype (ASR) to determine which types of resistance genes are effective: ASR and/or APR. Additionally, early identification of promising lines or parental candidates for breeding crosses is crucial to accelerate the development of wheat lines with durable YR resistance.

Despite Uruguay's longstanding wheat breeding program at the National Institute of Agronomical Research (INIA), which has focused on developing resistance to major regional diseases such as leaf (Silva et al. 2015) and stem rusts (Baraibar et al. 2020), Fusarium head blight, Septoria tritici blotch and tan spot, YR was historically considered a minor threat. Consequently, no breeding efforts specifically targeting YR resistance were implemented, leaving the genetic basis of resistance in the local germplasm largely unknown (Germán and Luizzi 2018). In Uruguay, the *PstS13* genetic group has been reported as the most prevalent since the 2017 epidemics (Riella et al. 2024). Within *PstS13*, the two races used in this study for field inoculations, *Triticale2015(a)* and its locally discovered variant, *Triticale2015b*, with additional virulence to *Yr17* and *Yr32*, have been the most prevalent in recent years. The original *PstS13* race, *Triticale2015*, was first reported in Europe in 2015, primarily affecting triticale and durum wheat (Hovmøller et al. 2018). Since 2017, *PstS13* has been the predominant genetic group in Argentina (Hovmøller et al. 2018, 2019; Carmona et al. 2019), it was also detected in Chile (Hovmøller et al. 2019) and more recently in Paraguay (Fernández-Gamarra et al. 2023).

Phenotypic Variation for Wheat Resistance to Yellow Rust

The panel of 366 wheat lines, including INIA germplasm and other commercial varieties widely used locally, was phenotyped in field trials over two consecutive years under artificial inoculations with the predominant *Pst* races. Additionally, seedling assays were performed with the same races used for field inoculations. Phenotypic data showed significant variation among lines for all evaluated traits. Seedling IT exhibited a bias toward susceptibility (**Fig. S2**), for the broader virulent race (*Triticale2015b*), conversely, field YR AUDPC showed a bias toward resistance, suggesting a low presence of effective ASR genes in the panel and the presence of APR genes, which are more effective in the adult plant stage. This is consistent with the panel composition, as many lines originate from crosses with sources of leaf rust APR (generally pleiotropic for YR APR), while no intentional introgressions of YR ASR genes have been performed in the WBP. Another evidence of absence of effective ASR genes in the panel is the lack of significant correlation between seedling IT and field AUDPC (r^2=0.46).

The high broad-sense heritability for AUDPC across 2021 (0.98), 2022 (0.98), and combined years (0.97), as an indicator of repeatability, coupled with strong correlations among replicates within each year (0.94–0.95) and between BLUEs AUDPC values across years (0.74), underscores the robustness of this phenotypic dataset for GWAS and GP analyses.Population Structure of the Wheat Panel

Accounting for population structure is critical in GWAS to minimize false-positive marker-trait associations (Pritchard et al. 2000; Yu et al. 2006; Zhu et al. 2008). In this study, population structure analyses revealed no strong genetic stratification among the 366 wheat lines that would require inclusion in subsequent GWAS analyses. Lines did not cluster based on origin (INIA-WBP, INIA-RGDP, or other breeding programs), likely reflecting the diverse germplasm and resistance sources used by INIA. Moreover, no clear association was observed between AUDPC values and line origin. Interestingly, lines from the INIA-RGDP, which were selected for APR to leaf rust, exhibited lower average YR AUDPC values than commercial varieties or advanced INIA-WBP lines. This observation suggests the presence of potentially pleiotropic APR genes in these lines, providing a valuable genetic resource for breeding wheat lines with enhanced YR resistance. Exploiting these genetic resources could accelerate the development of cultivars with durable, broad disease spectrum resistance.

Genome-Wide Association Study (GWAS)

The high-quality phenotypic data collected from the GWAS panel of 366 wheat lines evaluated in both field and greenhouse trials, combined with a dense set of SNPs distributed across the genome (**Fig. S4**), provided a robust framework for identifying genomic regions associated with YR resistance. As no strong population structure was found, the K model was enough to control for spurious associations, as confirmed by quantile-quantile (QQ) plots (**Fig. S9**).

Eight genomic regions associated with YR resistance were identified in field trials, with stable expression as these were consistently detected across data from both years (data not shown). Pyramiding the identified QTL for YR resistance significantly reduced YR AUDPC (**Fig. 3**), aligning with findings from other studies (Maccaferri et al. 2015; Zhou et al. 2021; Franco et al. 2022; Lin et al. 2023; Miedaner et al. 2024; Wang et al. 2024), which also highlight additive effects improving YR and leaf rust resistance as the number of favorable QTL increases.

GWAS analyses for seedling resistance did not identify any of the regions detected in the field. The two regions associated with seedling resistance for one of the *Pst* races were ineffective to the other race. While both races belong to the same genetic group, race *Triticale2015b* has additional virulence to *Yr17* and *Yr32* (Riella et al. 2024) which are located in distinct genomic regions from the QTL identified in field tests. These results confirm that the QTL identified in the field confer APR.

Analysis of identified genomic regions associated with yellow rust resistance

Eight genomic regions associated with YR resistance were identified: one on chromosome 1B, three on 2B separated by more than 126 Mb, two on 5B, one on 5D and one on 7B. Regions significantly associated with YR resistance identified in this study were compared with previously mapped *Yr* genes and QTL using the most updated atlas available (McIntosh 2024; Tong et al. 2024). The possibility that these associations were due to differences in heading date was excluded, since GWAS analyses using days to heading as the response variable revealed no overlap between the QTL associated with YR resistance and QTL associated to heading date (**Fig. S6 C**). Additionally, two QTL associated with seedling resistance to the *Pst* race *Triticale2015a* were identified on chromosomes 2D and 3A, but none were identified to race *Triticale2015b*, indicating that the resistance detected in the field was expressed after the seedling stage and is most possibly conferred by APR genes.

Adult-plant resistance QTL

Chromosome 1B

QYr.uy-1BL located on the long arm of chromosome 1B explained only 4.9% of the total variance, and had the lowest effect, reducing YR AUDPC by 848.8 (**Table 2**), which represents an average AUDPC reduction of 12% compared to the lines with the less favorable allele. This QTL was widely present in the lines (80%), predominantly in germplasm from INIA (**Table 3**). Chromosome 1B, is considered a hotspot for YR resistance, as at least eight *Yr* genes have been mapped on this chromosome, including *Yr9* (Lukaszewski 2000), *Yr10* (Liu et al. 2014), *Yr15* (Klymiuk et al. 2018), *Yr24*/*Yr26* (McIntosh 2024), *Yr29* (William et al. 2003), *Yr64* (Cheng et al. 2014), and *Yr65* (Cheng et al. 2014). Numerous other temporarily designated genes, such as *YrChk* (Liu et al. 2007), *YrExp1* (Lin and Chen 2007), and *YrGn22* (Li et al. 2016), are also located on 1B. However, all these genes have been mapped far from the *QYr.uy-1BL* region detected in our study. *Yr29*, a pleiotropic APR gene with a moderate effect, located on chromosome 1BL at 661.86 Mb (Li et al. 2020), is the closets among these *Yr* genes, but still lies more than 120 Mb away from *QYr.uy-1BL* region.. Genotyping of the panel using a KASP marker for *Yr29* (**Table S1**) revealed that it was present in 85% of the lines. However, *Yr29* did not show a significant effect on YR AUDPC. This evidence indicates that *QYr.uy-1BL* is not *Yr29*. In addition, over a dozen studies have reported QTL for YR resistance on this chromosome (Alemu et al. 2021; Draz et al. 2021). *QYr.uy-1BL* might correspond to the closest reported QTL located at approximately 8 Mb (Rosewarne et al. 2012) (**Table S3**).

Chromosome 2B

Three QTL were identified on the long arm of chromosome 2B. *QYr.uy-2BL.1* accounted for 5.7% of the total phenotypic variance, with an estimated effect of 706.7, corresponding to a 45.3% reduction in AUDPC relative to lines carrying the susceptible allele. The favorable allele of *QYr.uy-2BL.1* was present in 35% of the lines and was more frequently observed in germplasm from breeding programs

other than INIA (**Table 3**). *QYr.uy-2BL.2* explained 12.1% of the variance, with an estimated effect of -1268.2, corresponding to a 49% reduction in AUDPC. The favorable allele was detected in 18% of the lines, and was more prevalent in non-INIA cultivars (**Table 3**). *QYr.uy-2BL.3* had the largest effect among all QTL detected in this study, reducing YR AUDPC by 1425.2 (61%) and explaining 21.2% of the total variance (**Table 2**). The favorable allele was present in 27% of the lines (**Table 3**).

Several *Yr* genes, including *Yr5*, *Yr7* (Marchal et al. 2018), *Yr41* (Luo et al. 2008), *Yr43* (Feng et al. 2015), *Yr44* (Sui et al. 2009), *Yr53* (Xu et al. 2013), and *Yr72* (Chhetri et al. 2023), along with numerous temporarily designated genes and QTL, have been mapped to the long arm of chromosome 2B. Several loci associated with APR have also been identified on this chromosome. *QYr.uy-2BL.1*, located between 400.34 and 464.32 Mb, overlaps with two previously reported QTL: *QYr.caas-2BS.1* (Bai et al. 2012) and *QYr.ifa-2BL* (Buerstmayr et al. 2014) (**Table S3**). *QYr.uy-2BL.2*, located between 564.47 and 564.82 Mb, lies approximately 40 Mb from *Yr53*, which has not been introgressed into INIA-WBP germplasm. Two nearby QTL, *QYr.nafu-2BL* (Zhou et al. 2015) and *QYrqn.nwafu-2BL* (Zeng et al. 2019a) are located 8 Mb and 15 Mb away, respectively, and confer YR APR. Due to its low frequency in the panel *QYr.uy-2BL.*2 represents a QTL with potential from the breeding perspective.

The physical position of *QYr.uy-2BL.3* is close to ASR genes *Yr5*, *Yr7*, and *YrSP* which belong to a complex gene cluster (Marchal et al. 2018). *Yr7* and *YrSP* are ASR genes ineffective to the *Pst* races present in Uruguay (Riella et al. 2024) therefore these genes are not *QYr.uy-2BL.3*. Only ASE gene *Yr5* remains effective in Uruguay. Moreover, GWAS analyses of seedling ITs using the same *Pst* races as those used in field inoculations did not identify associations near the *Yr5* locus. Among lines carrying the favorable allele for *QYr.uy-2BL.3*, both resistant and susceptible seedling responses were observed, whereas the expected IT for *Yr5* carriers is 0; to ; (McIntosh et al. 1995). In race identification tests, *Avocet Yr5* which carries *Yr5* as the sole gene consistently showed an IT of 0 or 1 for both races. Additionally, KASP marker analysis (Marchal et al. 2018) indicated the absence of *Yr5* in the tested lines, including those carrying *QYr.uy-2BL.3* (data not shown). This evidence indicates that *QYr.uy-2BL.3* is not *Yr5*, but rather a distinct QTL associated with YR APR. QTL reported in this region, includ *QYrsnb.nwafu-2BL* (Zeng et al. 2019a) and *Qyr.gaas.2B.1* (Cheng et al. 2022), both located approximately 10 Mb from *QYr.uy-2BL.3* (**Table S3**). *QYr.uy-2BL.3* stands out as the most promising QTL for INIA-WBP due to its strong effect and relatively low frequency in the germplasm panel.Chromosome 5B

Two QTL were identified on chromosome 5B: *QYr.uy-5BS* on the short arm and *QYr.uy-5BL* on the long arm. *QYr.uy-5BS* explained 10.6% of the phenotypic variance, had an estimated effect of 973.2, corresponding to a 13.9% reduction in AUDPC relative to lines carrying the susceptible allele. The favorable allele of *QYr.uy-5BS* was present in 36% of the lines and was more frequently observed in germplasm from the INIA-RGDP program (**Table 3**). *QYr.uy-5BL* reduced YR AUDPC by 1156.8 (16%)

and accounted for 8.6% of the phenotypic variance (**Table 2**). It is present at high frequency (84%), with greater representation in INIA-RGDP (**Table 3**).

Two YR resistance genes have been previously reported on chromosome 5B: *Yr47* (Bansal et al. 2011) and *Yr19* (Chen et al. 1995). However, the genomic region of *Yr47* on the short arm of the chromosome is 64 Mb from *QYr.uy-5BS*. Therefore, *Yr47* is not any of the QTL reported in our study. *Yr19* is an ASR gene, whose physical position on chromosome 5B is not known (Chen et al. 1995). Since both *QYr.uy-5BS* and *QYr.uy-5BL* were detected only in our field trials but not at the seedling stage, they do not correspond *Yr19*.

The closest previously reported QTL to *QYr.uy-5BS* is *QYr.ufs-5B* (Agenbag et al. 2012) but is located more than 40 Mb away (**Table S3**). This strongly suggests that *QYr.uy-5BS* may represent a novel QTL which valuable for INIA-WBP and other breeding programs. Three QTL reported on chromosome 5BL, are located 10 Mb or less from *QYr.uy-5BL* (*QYr.YBZR-5BL*, Deng et al. 2022; *QYr.AYH-5BL*, Long et al. 2021; *QYrdr.wgp-5BL.2*, Hou et al. 2015). *QYr.uy-5BL* might be *QYrdr.wgp-5BL.2* which lies less than 1Mb from it.

Chromosome 5D

QYr.uy-5DL, located on the long arm of chromosome 5D, explained 7.3% of the phenotypic variance and reduced YR AUDPC by 898.4, representing a 14% average reduction compared to lines carrying the less favorable allele (**Table 2**). This QTL was detected in 75% of the lines, being been more frequently present in germplasm from INIA (**Table 3**). *Yr70* (Pasam et al. 2017), the only nominated gene located on this chromosome is over 200 Mb away. Two previously reported QTL, *QYrdr.wgp-5DL* (Hou et al. 2015) and *QYrbr.wpg-5D* (Case et al. 2014), have been identified on 5DL, at about 5 Mb from the region where *QYr.uy-5DL* is located (**Table S3**). It is present in high frequency in INIA germplasm, efforts should be made to maintain this QTL in the breeding germplasm.

Chromosome 7B

QYr.uy-7BL, located on the long arm of chromosome 7B, explained 6.6% of the phenotypic variance and reduced YR AUDPC by 777.2, corresponding to an average reduction of 12.7% compared to lines carrying the less favorable allele (**Table 2**). This QTL was present in 61% of the lines, with no major differences in frequency across germplasm origins (**Table 3**). *Yr67* (Bariana et al. 2022) has been reported approximately 40 Mb from the physical position of *QYr.uy-7BL*. QTL *QYr.hebau-7BL* (Zhang et al. 2019), *QYr.niab-7B* (Powell et al. 2013), and *QYr.cim-7BL* (Calvo-Salazar et al. 2015) colocalize with the region where *QYr.uy-7BL* is located (**Table S3**).

All-stage resistance QTL

QYr.uy-2DS

QYr.uy-2DS, identified for the *Triticale2015a* race, was the QTL with the largest effect at the seedling stage, explaining 19.1% of the phenotypic variance. Lines carrying the favorable allele for this QTL (20%) had an average IT of 2.4, representing a reduction of 2.3 IT units (49%) compared to the lines lacking it (**Table 2**). No *Yr* genes have been mapped to the region where *QYr.uy-2DS* is located, although the major QTL *Yrq1* (Cao et al. 2012) colocalize with *QYr.uy-2DS* and *QYr.hbau-2DS* (Gebrewahid et al. 2020) is only 3 Mb away (**Table S3**).

QYr.uy-3AL

QYr.uy-3AL was the QTL with the smallest effect in the seedling stage to race *Triticale2015a*, reducing IT in 1.4 (49%) and explaining 7.9% of the phenotypic variance (**Table 2**). *QYr.uy-3AL* was the most frequent seedling QTL within cultivars from breeding programs other than INIA (**Table 3**). *QYr.uy-3AL* is located on the long arm of chromosome 3A. *Yr76*, the only *Yr* gene previously mapped on chromosome 3A (Xiang et al. 2016), is located on the short arm, indicating that *QYr.uy-3AL* is distinct. Several QTL for YR resistance have also been reported on 3AL; among them, *QYr.nmbu.3A.2* (Lin et al. 2023) and *QYr.hbaas-3AL* (Jia et al. 2020), are the closest to *QYr.uy-3AL*, located approximately 7 and 12 Mb away, respectively (**Table S3**).

Both, *QYr.uy-2DS* and *QYr.uy-3AL*, are not effective to race *Triticale2015b* and were not detected in field tests, therefore their relevance for resistance breeding is limited.

Implication of identified QTL in the breeding program context

The identification of eight genomic regions associated with YR resistance in field trials and two regions in seedling assays highlights the value of exploring local genetic resources. Local breeding programs represent a valuable reservoir of genetic diversity adapted to local conditions and are key resources for breeding programs. While several ASR *Yr* genes remain effective to the current *Pst* population, the variability of the pathogen requires the continuous exploration and introgression of new resistance sources to increase the genetic diversity. *PstS13*, the predominant genetic group of *Pst* in local conditions, is virulent to several widely deployed *Yr* genes (Tadesse et al. 2014; Hovmøller et al. 2016). Other races within the *PstS13* group identified locally, acquired virulence to *Yr3*, *Yr17*, *Yr25*, *Yr27*, and *Yr32* (Riella et al. 2024).

Among the eight QTL identified in field trials, only *QYr.uy-2BL.3* co-localized with previously reported ASR *Yr* gene cluster (*Yr5*, *Yr7*, *YrSP*), but it was demonstrated it was not any of these genes. *QYr.uy-5BS* appears to be a novel QTL. Other QTL identified in this study are located near (10 Mb or less) of previously reported QTL, therefore, further confirmatory studies are required to determine whether these QTL correspond to known loci or represent new, distinct QTL, e.g. using markers for

679 QTL reported in the literature near those identified in this study as well as developing functional markers
680 and validating QTL through biparental populations.

681 The QTL identified in field trials were not detected in seedling tests (**Fig. S6**), indicating that
682 these correspond to APR genes. Their additive effects (**Fig. 3**) further support that these are likely race
683 non-specific and durable, which is expected within INIA germplasm, where ASR genes have not been
684 deliberately used. Many of the INIA-RGDP lines with low YR AUDPC are derived from crosses
685 between locally adapted materials and sources of leaf rust APR, mostly from CIMMYT. These lines
686 were selected for leaf rust resistance, suggesting a pleiotropic effect of the APR to both rusts. In that
687 sense, it would be expected that APR genes such as *Yr18*, *Yr29*, and *Yr46*, frequently present in
688 CIMMYT germplasm, or QTL for YR resistance found in this germplasm (Singh 1992; Singh and
689 Rajaram 1992, 1993) should have been detected in the GWAS analysis. However, genotype-by-
690 environment interactions involving minor APR genes might influence their expression, as previously
691 reported for rust diseases (Lillemo and Singh 2011; Calvo-Salazar et al. 2015; Silva et al. 2015).

692 KASP marker results revealed that *Yr18* was present in 28.7% of the lines (**Table S1**) and was
693 associated with a non-significant reduction in AUDPC (~307) which was not detected in the GWAS
694 analysis. One possible explanation is the low marker saturation of the D genome, particularly in the
695 region where *Yr18* resides (**Fig. S4**), which reflects the overall lower polymorphism of this genome
696 compared to the A and B genomes. To address this, GWAS was performed incorporating the KASP
697 marker for *Yr18* into the SNP matrix. However, the marker still did not surpass the significance threshold
698 in the updated models, suggesting that low marker density was not the cause of its non-detection.
699 Therefore, this result might be explained by the relatively small effect of *Yr18* in reducing AUDPC,
700 consistent with previous studies reporting partial resistance conferred by this gene (Wu et al. 2015; Zelba
701 et al. 2024). Similarly, *Yr29* was not detected by GWAS even after including its KASP marker in the
702 SNP matrix, despite showing a statistically significant AUDPC reduction (~349) (data not shown). Its
703 high frequency in the panel (present in 85% of lines) likely reduced the statistical power to detect
704 associations. Nevertheless, *Yr29* has been shown to have a stronger effect under Mexican field
705 conditions (Liu et al. 2022), suggesting that its effectiveness may be influenced by the environment. In
706 contrast, KASP marker results showed that *Yr46* was absent from the panel except for the check line
707 Thatcher *Yr46* (**Table S1**). Notably, this gene had a marked effect on disease resistance: Thatcher showed
708 an AUDPC of 4808, whereas Thatcher *Yr46* exhibited a much lower value (3315), highlighting the
709 potential of *Yr46* for introgression into INIA-WBP germplasm. However, its very low frequency in the
710 panel (<1%) prevented its detection in the GWAS, as it did not meet the MAF threshold used in this
711 study.A marked decrease in AUDPC was observed as the number of favorable QTL per line increased
712 (**Fig. 3**), indicating additive effects among the identified QTL. This highlights QTL pyramiding is a
713 promising strategy for breeding wheat with higher levels of durable resistance. Clearly, two of the QTL
714 (*QYr.uy-1BL* and *QYr.uy-5BL*) were already present at high proportion in the INIA-WBP advanced

germplasm and in cultivars of other origin. However, the other three QTL were present at much lower proportion and pyramiding them with those QTL already present may contribute to the development of YR resistant cultivars. Notably, the eleven lines carrying the favorable alleles for all eight QTL showed final disease severity values below 20%. Among them, two pre-breeding lines from the INIA program, R15F57341 and R17F57132, exhibited near-immunity levels at the adult plant stage, making them invaluable resources for resistance breeding and future research.

Genomic Prediction (GP)

Modern breeding programs, especially in a context where genotyping costs are increasingly affordable and accessible, require the optimization of strategies not only for selecting lines but also for efficiently identifying parents for crosses at an early stage. This is key to developing adapted and resistant cultivars in the shortest possible time. This study aimed to determine the predictive ability of different GP models using the genomic and phenotypic information of the panel lines. Additionally, it sought to demonstrate whether incorporating the presence of the QTL identified through GWAS for YR AUDPC as fixed effects could improve the GP models' predictive ability. Seven different GP models, which assume different distributions for marker effects, were evaluated. These models included A-BLUP model; RR-BLUP, which uses information from all markers; G-BLUP, which uses information about the genetic distance between lines to make predictions; and four types of Bayesian models: BA, BB, BC, and BL. The results of the comparison between the seven models showed no significant differences in performance between RR-BLUP and G-BLUP, with both models having correlations between observed and predicted AUDPC values close to 0.7, which is not suppressing given that the equivalence between these two models has been previously reported (Habier et al. 2007). No differences were observed with the Bayesian models BA, BB, or BC. In contrast, the BL model showed worse performance, with correlations between observed and predicted values around 0.5. BL results were similar to the A-BLUP model, which only uses the available pedigree relationships between the panel lines. Similar results, with minimal differences between prediction models for this disease, were reported by Tehseen et al. (2021) and Manickavelu et al. (2016). The G-BLUP and Bayesian models investigated in this study gave nearly identical prediction accuracies, despite assuming similar variances for all marker effects in the G-BLUP model, as reported by Tehseen et al. (2021). However, since no significant differences were observed between the regression-based G-BLUP and RR methods, and the Bayesian-based models, the assumption of marker effects having equal variances proved to be effective for YR AUDPC. Therefore, the higher computational time required for the prior densities and shrinkage of Bayesian models may not be necessary. G-BLUP or RR models have also been reported to offer similar prediction accuracies as the BC and BL methods for YR and stem rust (Ornella et al. 2012), stem rust (Rutkoski et al. 2014), and Fusarium head blight in wheat (Rutkoski et al. 2012).

GP proved to be efficient in predicting the response to YR within the GP panel, with prediction accuracies of around 0.7 for the equivalent models RR-BLUP and G-BLUP. The inclusion of GWAS-identified QTL as fixed effects in the G-BLUP model led to an improvement in prediction accuracy. Notably, the inclusion of the QTL with the highest effect was sufficient to achieve this improvement, as no further gains were observed when additional QTL were incorporated as fixed effects (**Fig. S8 A**). Moreover, the inclusion of fixed effects also impacted the MSE, which was reduced by 10.4% when *QYr.uy-2BL.3* was included, compared to the G-BLUP model without it (**Fig. S9 B**), likely due to their high effect on the response variable. In simulation studies it was demonstrated that modeling a large-effect locus as a fixed effect was advantageous when the heritability of the trait exceeded 0.5 and the locus explained more than 25% of the genetic variance (Bernardo 2014). Consequently, studies with real data have shown that G-BLUP models incorporating fixed-effect markers outperformed standard G-BLUP for traits where the fixed-effect markers explained a substantial proportion of the variation (Juliana et al. 2017). Similarly, Rutkoski et al. (2014) found that including fixed-effect markers in G-BLUP increased accuracy for quantitative APR to stem rust in wheat. This approach would maximize genetic gain only if GP was applied to the specific dataset used in their study. However, for new samples, outcomes from GP using G-BLUP alone could be just as favorable as those obtained by including fixed-effect linked markers.

Conclusions

The results of this study lay the foundation for understanding the genetic basis of the YR resistance present in a diverse wheat panel and can be directly applied to the development of new locally adapted cultivars with better YR resistance. We report eight genomic regions associated with field resistance, none of these regions were identified at seedling stage to race *Triticale2015b*. All loci conferred quantitative APR and did not correspond to known *Yr* genes. *QYr.uy-5BS* is most likely a novel QTL. The positions of the other seven QTL were close to previously reported QTL, further studies are needed to determine whether they represent known or novel QTL. Two QTL on 2D and 3A identified at the seedling stage to race *Triticale2015a* did not confer field resistance. Once validated, these QTL could be used to develop and select varieties with high levels of YR resistance. Similarly, GP was highly effective (with prediction ability around 0.7) in predicting disease levels, positioning GP as a valuable tool for selecting parents in breeding programs, as well as for selecting lines. The methodology used for analyzing both phenotypic field data and genotypic data enabled the identification of genomic regions associated with YR resistance and the evaluation of GP models which can be applicable to projects on other wheat diseases and crop species. Moreover, it proved to be highly robust and capable of delivering high-quality data, which serves as the foundation for any solid breeding strategy. These findings provide valuable insights into the genetic basis of YR and offer robust tools for enhancing YR resistance breeding efforts in wheat.

784 # References

785 Agenbag GM, Pretorius ZA, Boyd LA, et al (2012) Identification of adult plant resistance to stripe rust
786 in the wheat cultivar Cappelle-Desprez. Theoretical and Applied Genetics 125:109–120.
787 https://doi.org/10.1007/s00122-012-1819-5

788 Alemu A, Brazauskas G, Gaikpa DS, et al (2021) Genome-Wide Association Analysis and Genomic
789 Prediction for Adult-Plant Resistance to Septoria Tritici Blotch and Powdery Mildew in Winter
790 Wheat. Front Genet 12:1–15. https://doi.org/10.3389/fgene.2021.661742

791 Alexander DH, Novembre J, Lange K (2009) Fast model-based estimation of ancestry in unrelated
792 individuals. Genome Res 19:1655–1664. https://doi.org/10.1101/gr.094052.109

793 Ali S, Gladieux P, Leconte M, et al (2014) Origin, Migration Routes and Worldwide Population Genetic
794 Structure of the Wheat Yellow Rust Pathogen Puccinia striiformis f.sp. tritici. PLoS Pathog
795 10:e1003903. https://doi.org/10.1371/journal.ppat.1003903

796 Ayliffe M, Singh RP, Lagudah ES (2008) Durable resistance to wheat stem rust needed. Curr Opin Plant
797 Biol 11:187–192. https://doi.org/10.1016/j.pbi.2008.02.001

798 Bahri BA, Leconte M, Ouffroukh A, et al (2009) Geographic limits of a clonal population of wheat
799 yellow rust in the Mediterranean region. Mol Ecol 18:4165–4179. https://doi.org/10.1111/j.1365-
800 294X.2009.04267.x

801 Bai B, Ren Y, Xia X, et al (2012) Mapping of Quantitative Trait Loci for Adult Plant Resistance to Stripe
802 Rust in German Wheat Cultivar Ibis. J Integr Agric 11:528–536. https://doi.org/10.1016/S2095-
803 3119(12)60039-2

804 Bansal UK, Forrest KL, Hayden MJ, et al (2011) Characterisation of a new stripe rust resistance gene
805 Yr47 and its genetic association with the leaf rust resistance gene Lr52. Theoretical and Applied
806 Genetics 122:1461–1466. https://doi.org/10.1007/s00122-011-1545-4

807 Bao J, Malunga LN (2022) Editorial: Compositional Diversity in Cereals in Relation to Their Nutritional
808 Quality and Health Benefits. Front Nutr 8:2021–2022. https://doi.org/10.3389/fnut.2021.819923

809 Baraibar S, García R, Silva P, et al (2020) QTL mapping of resistance to Ug99 and other stem rust
810 pathogen races in bread wheat. Molecular Breeding 40:82. https://doi.org/10.1007/s11032-020-
811 01153-5

812 Bariana H, Kant L, Qureshi N, et al (2022) Identification and Characterisation of Stripe Rust Resistance
813 Genes Yr66 and Yr67 in Wheat Cultivar VL Gehun 892. Agronomy 12:.
814 https://doi.org/10.3390/agronomy12020318

Bassi FM, Bentley AR, Charmet G, et al (2016) Breeding schemes for the implementation of genomic selection in wheat (Triticum spp.). Plant Science 242:23–36. https://doi.org/10.1016/j.plantsci.2015.08.021

Bates D, Mächler M, Bolker B, Walker S (2015) Fitting Linear Mixed-Effects Models Using lme4. J Stat Softw 67:. https://doi.org/10.18637/jss.v067.i01

Bernardo R (2008) Molecular markers and selection for complex traits in plants: Learning from the last 20 years. Crop Sci 48:1649–1664. https://doi.org/10.2135/cropsci2008.03.0131

Bernardo R (2016) Bandwagons I, too, have known. Theoretical and Applied Genetics 129:2323–2332. https://doi.org/10.1007/s00122-016-2772-5

Bernardo R (2014) Genomewide Selection when Major Genes Are Known. Crop Sci 54:68–75. https://doi.org/10.2135/cropsci2013.05.0315

Bhavani S, Singh RP, Argillier O, et al (2011) Mapping durable adult plant stem rust resistance to the race Ug99 group in six CIMMYT wheats. In: Proceedings Borlaug Global Rust Initiative, 2011 Technical Workshop, 13-16 June, St. Paul, Minnesota, USA,. pp 44–53

Boden SA, McIntosh RA, Uauy C, et al (2023) Updated guidelines for gene nomenclature in wheat. Theoretical and Applied Genetics 136:1–16. https://doi.org/10.1007/s00122-023-04253-w

Boerger A (1934) Consideraciones restropectivas acerca de la primera aparición epidémica de la roya amarilla (Puccinia glumarum (Schm) Erikss. et Henn.) en el Río de la Plata. Revista del Ministerio de Industrias (Montevideo) 1:5–16

Bouvet L, Holdgate S, James L, et al (2022) The evolving battle between yellow rust and wheat: implications for global food security. Theoretical and Applied Genetics 135:741–753. https://doi.org/10.1007/s00122-021-03983-z

Brachi B, Faure N, Horton M, et al (2010) Linkage and association mapping of Arabidopsis thaliana flowering time in nature. PLoS Genet 6:40. https://doi.org/10.1371/journal.pgen.1000940

Browning BL, Zhou Y, Browning SR (2018) A One-Penny Imputed Genome from Next-Generation Reference Panels. Am J Hum Genet 103:338–348. https://doi.org/10.1016/j.ajhg.2018.07.015

Buerstmayr M, Matiasch L, Mascher F, et al (2014) Mapping of quantitative adult plant field resistance to leaf rust and stripe rust in two European winter wheat populations reveals co-location of three QTL conferring resistance to both rust pathogens. Theoretical and Applied Genetics 127:2011–2028. https://doi.org/10.1007/s00122-014-2357-0

845 Calvo-Salazar V, Singh RP, Huerta-Espino J, et al (2015) Genetic analysis of resistance to leaf rust and
846 yellow rust in spring wheat cultivar Kenya Kongoni. Plant Dis 99:1153–1160.
847 https://doi.org/10.1094/PDIS-07-14-0718-RE

848 Campos P (2020) Estado de Situación de las royas de trigo en Argentina. Campaña 2019. 2020.

849 Campos P, Formento N, Couretot L, Alberione E (2016) Aparición epifítica de roya amarilla del trigo
850 en la región pampeana argentina. 1–5

851 Cao X, Zhou J, Gong X, et al (2012) Identification and Validation of a Major Quantitative Trait Locus
852 for Slow-rusting Resistance to Stripe Rust in Wheat. J Integr Plant Biol 54:330–344.
853 https://doi.org/10.1111/j.1744-7909.2012.01111.x

854 Carmona MA, Sautua FJ, Pérez-Hernández O, et al (2019) Rapid emergency response to yellow rust
855 epidemics caused by newly introduced lineages of Puccinia striiformis f. sp. tritici in Argentina.
856 Trop Plant Pathol 44:385–391. https://doi.org/10.1007/s40858-019-00295-y

857 Case AJ, Naruoka Y, Chen X, et al (2014) Mapping Stripe Rust Resistance in a BrundageXCoda Winter
858 Wheat Recombinant Inbred Line Population. PLoS One 9:.
859 https://doi.org/10.1371/journal.pone.0091758

860 Cerrudo D, Cao S, Yuan Y, et al (2018) Genomic selection outperforms marker assisted selection for
861 grain yield and physiological traits in a maize doubled haploid population across water treatments.
862 Front Plant Sci 9:1–12. https://doi.org/10.3389/fpls.2018.00366

863 Chen X (2013) Review Article: High-Temperature Adult-Plant Resistance, Key for Sustainable Control
864 of Stripe Rust. Am J Plant Sci 04:608–627. https://doi.org/10.4236/ajps.2013.43080

865 Chen XM (2005) Epidemiology and control of stripe rust [Puccinia striiformis f. sp. tritici] on wheat.
866 Canadian Journal of Plant Pathology 27:314–337. https://doi.org/10.1080/07060660509507230

867 Chen XM, Jones SS, Line RF (1995) Chromosomal Location of Genes for Stripe Rust Resistance in
868 Spring Wheat Cultivars Compair, Fielder, Lee, and Lemhi and Interactions of Aneuploid Wheats
869 with Races of Puccinia striiformis. Phytopathology 85:375. https://doi.org/10.1094/Phyto-85-375

870 Cheng B, Gao X, Cao N, et al (2022) QTL mapping for adult plant resistance to wheat stripe rust in
871 M96-5 × Guixie 3 wheat population. J Appl Genet 63:265–279. https://doi.org/10.1007/s13353-
872 022-00686-z

873 Cheng P, Xu LS, Wang MN, et al (2014) Molecular mapping of genes Yr64 and Yr65 for stripe rust
874 resistance in hexaploid derivatives of durum wheat accessions PI 331260 and PI 480016.
875 Theoretical and Applied Genetics 127:2267–2277. https://doi.org/10.1007/s00122-014-2378-8

876 Chhetri M, Miah H, Wong D, et al (2023) Mapping of a Stripe Rust Resistance Gene Yr72 in the
877 Common Wheat Landraces AUS27506 and AUS27894 from the Watkins Collection. Genes
878 (Basel) 14:. https://doi.org/10.3390/genes14111993

879 Crossa J, Pérez-Rodríguez P, Cuevas J, et al (2017) Genomic Selection in Plant Breeding: Methods,
880 Models, and Perspectives. Trends Plant Sci 22:961–975.
881 https://doi.org/10.1016/j.tplants.2017.08.011

882 Daetwyler HD, Bansal UK, Bariana HS, et al (2014) Genomic prediction for rust resistance in diverse
883 wheat landraces. Theoretical and Applied Genetics 127:1795–1803.
884 https://doi.org/10.1007/s00122-014-2341-8

885 Deng M, Long L, Cheng Y, et al (2022) Mapping a stable adult-plant stripe rust resistance QTL on
886 chromosome 6AL in Chinese wheat landrace Yibinzhuermai. Crop Journal 10:1111–1119.
887 https://doi.org/10.1016/j.cj.2021.10.011

888 Di Rienzo JA, Casanoves F, González LA, et al (2009) Estadística para las ciencias agropecuarias, 6ta
889 edició. Córdoba, Brujas

890 Dray S, Dufour AB (2007) The ade4 package: Implementing the duality diagram for ecologists. J Stat
891 Softw 22:1–20. https://doi.org/10.18637/jss.v022.i04

892 Draz IS, Serfling A, Muqaddasi QH, Röder MS (2021) Quantitative trait loci for yellow rust resistance
893 in spring wheat doubled haploid populations developed from the German Federal ex situ genebank
894 genetic resources. Plant Genome 14:1–16. https://doi.org/10.1002/tpg2.20142

895 Dreisigacker S, D. S, A.E. RJ, et al (2016) CIMMYT Wheat Molecular Genetics: Laboratory Protocols
896 and Applications to Wheat Breeding

897 Feng JY, Wang MN, Chen XM, et al (2015) Molecular mapping of YrSP and its relationship with other
898 genes for stripe rust resistance in wheat chromosome 2BL. Phytopathology 105:1206–1213.
899 https://doi.org/10.1094/PHYTO-03-15-0060-R

900 Fernández-Gamarra MA, Chávez P, Cardozo Téllez L, et al (2023) First Report of Yellow Rust (Puccinia
901 striiformis f. sp. tritici) in Wheat (Triticum aestivum) in Paraguay. Plant Dis 107:558.
902 https://doi.org/https://doi.org/10.1094/PDIS- 03-22-0482-PDN

903 Flor HH (1955) Host-parasite interaction in flax rust-its genetics and other implications. Palynology
904 45:680–685

905 Forrest K, Pujol V, Bulli P, et al (2014) Development of a SNP marker assay for the Lr67 gene of wheat
906 using a genotyping by sequencing approach. Molecular Breeding 34:2109–2118.
907 https://doi.org/10.1007/s11032-014-0166-4

908 Franco MF, Polacco AN, Campos P, et al (2022) Genome-wide association study for resistance in bread
909 wheat (Triticum aestivum L.) to stripe rust (Puccinia striiformis f. sp. tritici) races in Argentina.
910 BMC Plant Biol 22:1–17. https://doi.org/10.1186/s12870-022-03916-y

911 Gebrewahid TW, Zhou Y, Zhang P, et al (2020) Mapping of stripe rust and leaf rust resistance
912 quantitative trait loci in the Chinese spring wheat line Mianyang351-15. Phytopathology
913 110:1074–1081. https://doi.org/10.1094/PHYTO-08-19-0316-R

914 Germán SE, Azzimonti G, Castro M, et al (2018) Roya estriada de trigo: epidemia en 2017 asociada a
915 la presencia de razas agresivas del patógeno y sus posibles consecuencias. Revista INIA-Nº 54 36–
916 41

917 Germán SE, Barcellos A, Chaves M, et al (2007) The situation of common wheat rusts in the Southern
918 Cone of America and perspectives for control. Aust J Agric Res 58:620–630.
919 https://doi.org/10.1071/AR06149

920 Germán SE, Caffarel J (1999) Roya estriada de trigo. Jornada de Cultivos de Invierno. INIA La
921 Estanzuela, Colonia, Uruguay. Serie Actividades de Difusión No. 188 25–32

922 Germán SE, Luizzi D (2018) 100 años de mejoramiento de trigo en INIA La Estanzuela. INIA,
923 Montevideo

924 Glaubitz JC, Casstevens TM, Lu F, et al (2014) TASSEL-GBS: A High Capacity Genotyping by
925 Sequencing Analysis Pipeline. PLoS One 9:e90346. https://doi.org/10.1371/journal.pone.0090346

926 Gutiérrez L, Germán SE, Pereyra S, et al (2015) Multi-environment multi-QTL association mapping
927 identifies disease resistance QTL in barley germplasm from Latin America. Theoretical and
928 Applied Genetics 128:501–516. https://doi.org/10.1007/s00122-014-2448-y

929 Habier D, Fernando RL, Dekkers JCM (2007) The impact of genetic relationship information on
930 genome-assisted breeding values. Genetics 177:2389–2397.
931 https://doi.org/10.1534/genetics.107.081190

932 Heffner EL, Sorrells ME, Jannink JL (2009) Genomic selection for crop improvement. Crop Sci 49:1–
933 12. https://doi.org/10.2135/cropsci2008.08.0512

934 Hou L, Chen X, Wang M, et al (2015) Mapping a large number of QTL for durable resistance to stripe
935 rust in winter wheat druchamp using SSR and SNP markers. PLoS One 10:1–24.
936 https://doi.org/10.1371/journal.pone.0126794

937 Hovmøller MS, Rodriguez-Algaba J, Thach T, et al (2018) Report for Puccinia striiformis race analyses
938 and molecular genotyping 2017. Slagelse

939 Hovmøller MS, Rodriguez-Algaba J, Thach T, et al (2019) Report for Puccinia striiformis race
940 analyses/molecular genotyping. Slagelse

941 Hovmøller MS, Sørensen CK, Walter S, Justesen AF (2011) Diversity of Puccinia striiformis on Cereals
942 and Grasses. Annu Rev Phytopathol 49:197–217. https://doi.org/10.1146/annurev-phyto-072910-
943 095230

944 Hovmøller MS, Thach T, Justesen AF (2023) Global dispersal and diversity of rust fungi in the context
945 of plant health. Curr Opin Microbiol 71:102243. https://doi.org/10.1016/j.mib.2022.102243

946 Hovmøller MS, Walter S, Bayles RA, et al (2016) Replacement of the European wheat yellow rust
947 population by new races from the centre of diversity in the near-Himalayan region. Plant Pathol
948 65:402–411. https://doi.org/10.1111/ppa.12433

949 Hovmøller MS, Yahyaoui AH, Milus EA, Justesen AF (2008) Rapid global spread of two aggressive
950 strains of a wheat rust fungus. Mol Ecol 17:3818–3826. https://doi.org/10.1111/j.1365-
951 294X.2008.03886.x

952 Jannink JL, Lorenz AJ, Iwata H (2010) Genomic selection in plant breeding: From theory to practice.
953 Brief Funct Genomic Proteomic 9:166–177. https://doi.org/10.1093/bfgp/elq001

954 Jia M, Yang L, Zhang W, et al (2020) Genome-wide association analysis of stripe rust resistance in
955 modern Chinese wheat. BMC Plant Biol 20:1–13. https://doi.org/10.1186/s12870-020-02693-w

956 Juliana P, Singh RP, Singh PK, et al (2017) Genomic and pedigree-based prediction for leaf, stem, and
957 stripe rust resistance in wheat. Theoretical and Applied Genetics 130:1415–1430.
958 https://doi.org/10.1007/s00122-017-2897-1

959 Kema GHJ (1992) Resistance in spelt wheat to yellow rust - III. Phylogenetical considerations.
960 Euphytica 63:225–231. https://doi.org/10.1007/BF00024548

961 Klymiuk V, Yaniv E, Huang L, et al (2018) Cloning of the wheat Yr15 resistance gene sheds light on the
962 plant tandem kinase-pseudokinase family. Nat Commun 9:. https://doi.org/10.1038/s41467-018-
963 06138-9

964 Li J, Dundas I, Dong C, et al (2020) Identification and characterization of a new stripe rust resistance
965 gene Yr83 on rye chromosome 6R in wheat. Theoretical and Applied Genetics 133:1095–1107.
966 https://doi.org/10.1007/s00122-020-03534-y

967 Li Q, Ma D, Li Q, et al (2016) Genetic Analysis and Molecular Mapping of a Stripe Rust Resistance
968 Gene in Chinese Wheat Differential Guinong 22. Journal of Phytopathology 164:476–484.
969 https://doi.org/10.1111/jph.12473

970 Lillemo M, Singh RP, William M et al. (2011) Multiple rust resistance and gene additivity in wheat:
971 Lessons from multi-location case studies in cultivars Parula and Saar. In: Proceedings Borlaug
972 Global Rust Initiative, 2011 Technical Workshop, St. Paul, 13–16 June,. p pp 111–120

973 Lin F, Chen XM (2007) Genetics and molecular mapping of genes for race-specific all-stage resistance
974 and non-race-specific high-temperature adult-plant resistance to stripe rust in spring wheat cultivar
975 Alpowa. Theoretical and Applied Genetics 114:1277–1287. https://doi.org/10.1007/s00122-007-
976 0518-0

977 Lin M, Dieseth JA, Alsheikh M, et al (2023) A major yellow rust resistance QTL on chromosome 6A
978 shows increased frequency in recent Norwegian spring wheat cultivars and breeding lines.
979 Theoretical and Applied Genetics 136:1–15. https://doi.org/10.1007/s00122-023-04397-9

980 Listgarten J, Lippert C, Kadie CM, et al (2012) Improved linear mixed models for genome-wide
981 association studies. Nat Methods 9:525–526. https://doi.org/10.1038/nmeth.2037

982 Liu D, Yuan C, Singh RP, et al (2022) Stripe rust and leaf rust resistance in CIMMYT wheat line
983 "Mucuy" is conferred by combinations of race-specific and adult-plant resistance loci. Front Plant
984 Sci 13:. https://doi.org/10.3389/fpls.2022.880138

985 Liu F, Niu Y, Deng H, Tan G (2007) Mapping of a Major Stripe Rust Resistance Gene in Chinese Native
986 Wheat Variety Chike Using Microsatellite Markers. Journal of Genetics and Genomics 34:1123–
987 1130. https://doi.org/10.1016/S1673-8527(07)60128-3

988 Liu W, Frick M, Huel R, et al (2014) Wheat Yr10 Encodes a Unique CC-NBS-LRR Sequence Stripe
989 Rust Resistance Gene Yr10 Encodes an Evolutionary-conserved and Unique CC-NBS-LRR
990 Sequence in Wheat R6M 1Y5 4 Retired from Agriculture and Agri-Food Canada Downloaded
991 from. Molecular Plant Advance Access 26:

992 Long L, Yao F, Guan F, et al (2021) A Stable Quantitative Trait Locus on Chromosome 5BL Combined
993 with Yr18 Conferring High-Level Adult Plant Resistance to Stripe Rust in Chinese Wheat
994 Landrace Anyuehong. Phytopathology 111:1594–1601. https://doi.org/10.1094/PHYTO-10-20-
995 0465-R

996 Lorenz AJ, Chao S, Asoro FG, et al (2011) Genomic Selection in Plant Breeding. Knowledge and
997 Prospects., 1st edn. Elsevier Inc.

998 Lukaszewski AJ (2000) Manipulation of the 1RS.1BL translocation in wheat by induced homoeologous
999 recombination. Crop Sci 40:216–225. https://doi.org/10.2135/cropsci2000.401216x

1000 Luo PG, Hu XY, Ren ZL, et al (2008) Allelic analysis of stripe rust resistance genes on wheat
1001 chromosome 2BS. Genome 51:922–927. https://doi.org/10.1139/G08-079

1002 Maccaferri M, Zhang J, Bulli P, et al (2015) A genome-wide association study of resistance to stripe rust
1003 (Puccinia striiformis f. sp. tritici) in a worldwide collection of hexaploid spring wheat (Triticum
1004 aestivum L.). Genes, Genomes, Genetics 5:449–465. https://doi.org/10.1534/g3.114.014563

1005 Manickavelu A, Joukhadar R, Jighly A, et al (2016) Genome wide association mapping of stripe rust
1006 resistance in Afghan wheat landraces. Plant Science 252:222–229.
1007 https://doi.org/10.1016/j.plantsci.2016.07.018

1008 Marchal C, Zhang J, Zhang P, et al (2018) BED-domain-containing immune receptors confer diverse
1009 resistance spectra to yellow rust. Nat Plants 4:662–668. https://doi.org/10.1038/s41477-018-0236-
1010 4

1011 Mayor PJ, Bernardo R (2009) Genomewide selection and marker-assisted recurrent selection in doubled
1012 haploid versus F2 populations. Crop Sci 49:1719–1725.
1013 https://doi.org/10.2135/cropsci2008.10.0587

1014 McIntosh RA (2024) Wheat Gene Catalogue. In: GrainGenes.
1015 https://wheat.pw.usda.gov/GG3/content/october-2024-wheat-gene-catalogue-2024-released-
1016 covering-all-wgc-curations

1017 McIntosh RA, Wellings CR, Park RF (1995) Wheat Rusts: An Atlas of Resistance Genes. CSIRO
1018 Publications

1019 McNeal FH, Konzak CF, Smith EP, et al (1971) A uniform system for recording and processing cereal
1020 research data. US Dept Agric Res Serv ARS 34:121–143

1021 Miedaner T, Afzal M, Longin CF (2024) Genome-wide association study for resistances to yellow rust,
1022 powdery mildew, and Septoria tritici blotch in cultivated emmer. Euphytica 220:1–19.
1023 https://doi.org/10.1007/s10681-024-03296-4

1024 Milus EA, Kristensen K, Hovmøller MS (2009) Evidence for increased aggressiveness in a recent
1025 widespread strain of Puccinia striiformis f. sp. tritici causing stripe rust of wheat. Phytopathology
1026 99:89–94. https://doi.org/10.1094/PHYTO-99-1-0089

1027 Milus EA, Seyran E, McNew R (2006) Aggressiveness of Puccinia striiformis f. sp. tritici isolates in the
1028 south-central United States. Plant Dis 90:847–852. https://doi.org/10.1094/PD-90-0847

1029 Mrode RA (2014) Linear models for the prediction of animal breeding values, 3rd Editio. CABI, Boston,
1030 MA

1031 Muleta KT, Bulli P, Zhang Z, et al (2017) Unlocking Diversity in Germplasm Collections via Genomic
1032 Selection: A Case Study Based on Quantitative Adult Plant Resistance to Stripe Rust in Spring
1033 Wheat. Plant Genome 10:1–15. https://doi.org/10.3835/plantgenome2016.12.0124

1034 Ornella L, González-Camacho JM, Dreisigacker S, Crossa J (2017) Wheat Rust Diseases. Springer New
1035 York, New York, NY

1036 Ornella L, Singh S, Perez P, et al (2012) Genomic Prediction of Genetic Values for Resistance to Wheat
1037 Rusts. Plant Genome 5:. https://doi.org/10.3835/plantgenome2012.07.0017

1038 Pasam RK, Bansal UK, Daetwyler HD, et al (2017) Detection and validation of genomic regions
1039 associated with resistance to rust diseases in a worldwide hexaploid wheat landrace collection
1040 using BayesR and mixed linear model approaches. Theoretical and Applied Genetics 130:777–
1041 793. https://doi.org/10.1007/s00122-016-2851-7

1042 Pérez P, De Los Campos G (2014) Genome-wide regression and prediction with the BGLR statistical
1043 package. Genetics 198:483–495. https://doi.org/10.1534/genetics.114.164442

1044 Poland J, Rutkoski J (2016) Advances and Challenges in Genomic Selection for Disease Resistance.
1045 Annu Rev Phytopathol 54:79–98. https://doi.org/10.1146/annurev-phyto-080615-100056

1046 Powell NM, Lewis CM, Berry ST, et al (2013) Stripe rust resistance genes in the UK winter wheat
1047 cultivar Claire. Theoretical and Applied Genetics 126:1599–1612. https://doi.org/10.1007/s00122-
1048 013-2077-x

1049 Pritchard JK, Stephens M, Donnelly P (2000) Inference of Population Structure Using Multilocus
1050 Genotype Data. Genetics 155:945–959. https://doi.org/10.1093/genetics/155.2.945

1051 R Core Team (2024) R: A Language and Environment for Statistical Computing

1052 Rajaram S, Campos A (1974) Epidemiology of wheat rusts in the western hemisphere. CIMMYT
1053 Research Bulletin 27

1054 Rasheed A, Wen W, Gao F, et al (2016) Development and validation of KASP assays for genes
1055 underpinning key economic traits in bread wheat. Theoretical and Applied Genetics 129:1843–
1056 1860. https://doi.org/10.1007/s00122-016-2743-x

1057 Remington DL, Thornsberry JM, Matsuoka Y, et al (2001) Structure of linkage disequilibrium and
1058 phenotypic associations in the maize genome. Proc Natl Acad Sci U S A 98:11479–11484.
1059 https://doi.org/10.1073/pnas.201394398

1060 Riella V, Rodriguez-Algaba J, García R, et al (2024) New races with wider virulence indicate rapid
1061 evolution of Puccinia striiformis f. sp. tritici in the Southern Cone of America. Plant Dis.
1062 https://doi.org/10.1094/pdis-02-24-0320-re

1063 Rosewarne GM, Herrera-Foessel SA, Singh RP, et al (2013) Quantitative trait loci of stripe rust
1064 resistance in wheat. Theoretical and applied genetics 126:2427–2449.
1065 https://doi.org/10.1007/s00122-013-2159-9

1066 Rosewarne GM, Singh RP, Huerta-Espino J, et al (2012) Analysis of leaf and stripe rust severities reveals
1067 pathotype changes and multiple minor QTLs associated with resistance in an Avocet × Pastor
1068 wheat population. Theoretical and Applied Genetics 124:1283–1294.
1069 https://doi.org/10.1007/s00122-012-1786-x

1070 Rosyara UR, De Jong WS, Douches DS, Endelman JB (2016) Software for Genome-Wide Association
1071 Studies in Autopolyploids and Its Application to Potato. Plant Genome 9:1–10.
1072 https://doi.org/10.3835/plantgenome2015.08.0073

1073 Rudolf W, Job M (1931) La existencia de Puccinia glumarum tritici (Schmidt) Erikss. et Henn. en los
1074 países del Rio de la Plata. Arch Soc Biol Montevideo 5:1363:1370

1075 Rutkoski J, Benson J, Jia Y, et al (2012) Evaluation of Genomic Prediction Methods for Fusarium Head
1076 Blight Resistance in Wheat. Plant Genome 5:51–61.
1077 https://doi.org/10.3835/plantgenome2012.02.0001

1078 Rutkoski J, Heffner EL, Sorrells ME (2011) Genomic selection for durable stem rust resistance in wheat.
1079 Euphytica 179:161–173. https://doi.org/10.1007/s10681-010-0301-1

1080 Rutkoski J, Poland J, Mondal S, et al (2016) Canopy temperature and vegetation indices from high-
1081 throughput phenotyping improve accuracy of pedigree and genomic selection for grain yield in
1082 wheat. G3: Genes, Genomes, Genetics 6:2799–2808. https://doi.org/10.1534/g3.116.032888

1083 Rutkoski J, Poland J, Singh RP, et al (2014) Genomic Selection for Quantitative Adult Plant Stem Rust
1084 Resistance in Wheat. Plant Genome 7:1–10. https://doi.org/10.3835/plantgenome2014.02.0006

1085 Rutkoski J, Singh RP, Huerta-Espino J, et al (2015) Efficient Use of Historical Data for Genomic
1086 Selection: A Case Study of Stem Rust Resistance in Wheat. Plant Genome 8:1–10.
1087 https://doi.org/10.3835/plantgenome2014.09.0046

1088 Saghai-Maroof MA, Soliman KM, Jorgensen RA, Allard RW (1984) Ribosomal DNA spacer-length
1089 polymorphisms in barley: mendelian inheritance, chromosomal location, and population dynamics.
1090 Proc Natl Acad Sci U S A 81:8014–8018. https://doi.org/10.1073/pnas.81.24.8014

1091 Schmid M, Bennewitz J (2017) Invited review: Genome-wide association analysis for quantitative traits
1092 in livestock - A selective review of statistical models and experimental designs. Arch Anim Breed
1093 60:335–346. https://doi.org/10.5194/aab-60-335-2017

1094 Silva P, Calvo-Salazar V, Condón F, et al (2015) Effects and interactions of genes Lr34, Lr68 and Sr2
1095 on wheat leaf rust adult plant resistance in Uruguay. Euphytica 204:599–608.
1096 https://doi.org/10.1007/s10681-014-1343-6

Silva P, Riella V, García R, et al (2023) Roya estriada de trigo: una nueva realidad para el cultivo avances en el conocimiento para un manejo adecuado. Revista INIA-Nº 73 31–35

Singh RP (1992) Genetic Association of Leaf Rust Resistance Gene Lr34 with Adult Plant Resistance to Stripe Rust in Bread Wheat. Phytopathology 82:835. https://doi.org/10.1094/Phyto-82-835

Singh RP, Hodson DP, Huerta-Espino J, et al (2011) The emergence of Ug99 races of the stem rust fungus is a threat to world wheat production. Annu Rev Phytopathol 49:465–481. https://doi.org/10.1146/annurev-phyto-072910-095423

Singh RP, Huerta-Espino J, Rajaram S (2000) Achieving near-immunity to leaf and stripe rusts in wheat by combining slow rusting resistance genes. Acta Phytopathol Entomol Hung 35:133–139

Singh RP, Rajaram S (1992) Genetics of adult-plant resistance of leaf rust in "frontana" and three CIMMYT wheats. Genome 35:24–31. https://doi.org/10.1139/g92-004

Singh RP, Rajaram S (1993) Genetics of adult plant resistance to stripe rust in ten spring bread wheats. Euphytica 72:1–7. https://doi.org/10.1007/BF00023766

Sørensen CK, Hovmøller MS, Leconte M, et al (2014) New Races of Puccinia striiformis Found in Europe Reveal Race Specificity of Long-Term Effective Adult Plant Resistance in Wheat. Phytopathology 104:1042–1051. https://doi.org/10.1094/PHYTO-12-13-0337-R

Sui XX, Wang MN, Chen XM (2009) Molecular Mapping of a Stripe Rust Resistance Gene in Spring Wheat Cultivar Zak. Phytopathology 99:1209–1215. https://doi.org/10.1094/PHYTO-99-10-1209

Tadesse W, Ogbonnaya FC, Jighly A, et al (2014) Association mapping of resistance to yellow rust in winter wheat cultivars and elite genotypes. Crop Sci 54:607–616. https://doi.org/10.2135/cropsci2013.05.0289

Tehseen MM, Kehel Z, Sansaloni CP, et al (2021) Comparison of Genomic Prediction Methods for Yellow, Stem, and Leaf Rust Resistance in Wheat Landraces from Afghanistan. Plants 10:558. https://doi.org/10.3390/plants10030558

Tong J, Zhao C, Liu D, et al (2024) Genome-wide atlas of rust resistance loci in wheat. Theoretical and Applied Genetics 137:1–16. https://doi.org/10.1007/s00122-024-04689-8

Vallega J (1938) Dos nuevas selecciones de trigo de origen hibrido inmunes a "Puccinia glumarum." Revista de la Facultad de Agronomía (La Plata) 22:139–145

Wallace JG, Larsson SJ, Buckler ES (2014) Entering the second century of maize quantitative genetics. Heredity (Edinb) 112:30–38. https://doi.org/10.1038/hdy.2013.6

1127 Wang W, Jin P, Zhang J, et al (2024) Favorable Loci Identified for Stripe Rust Resistance in Chinese
1128 Winter Wheat Accessions via Genome-Wide Association Study. Plant Dis 108:71–81.
1129 https://doi.org/10.1094/PDIS-12-22-2842-RE

1130 Wellings CR (2007) Puccinia striiformis in Australia: A review of the incursion, evolution, and
1131 adaptation of stripe rust in the period 1979-2006. Aust J Agric Res 58:567–575.
1132 https://doi.org/10.1071/AR07130

1133 William HM, Singh RP, Huerta-Espino J, et al (2003) Molecular marker mapping of leaf rust resistance
1134 gene Lr46 and its association with stripe rust resistance gene Yr29 in wheat. Phytopathology
1135 93:153–159. https://doi.org/10.1094/PHYTO.2003.93.2.153

1136 Wolak ME (2012) nadiv : an R package to create relatedness matrices for estimating non-additive
1137 genetic variances in animal models. Methods Ecol Evol 3:792–796. https://doi.org/10.1111/j.2041-
1138 210X.2012.00213.x

1139 Wu L, Xia X, Rosewarne GM, et al (2015) Stripe rust resistance gene Yr18 and its suppressor gene in
1140 Chinese wheat landraces. Plant Breeding 134:634–640. https://doi.org/10.1111/pbr.12311

1141 Xiang C, Feng JY, Wang MN, et al (2016) Molecular mapping of stripe rust resistance gene Yr76 in
1142 winter club wheat cultivar tyee. Phytopathology 106:1186–1193. https://doi.org/10.1094/PHYTO-
1143 01-16-0045-FI

1144 Xu LS, Wang MN, Cheng P, et al (2013) Molecular mapping of Yr53, a new gene for stripe rust
1145 resistance in durum wheat accession PI 480148 and its transfer to common wheat. Theoretical and
1146 Applied Genetics 126:523–533. https://doi.org/10.1007/s00122-012-1998-0

1147 Yang J, Zaitlen NA, Goddard ME, et al (2014) Advantages and pitfalls in the application of mixed-
1148 model association methods. Nat Genet 46:100–106. https://doi.org/10.1038/ng.2876

1149 Yu J, Pressoir G, Briggs WH, et al (2006) A unified mixed-model method for association mapping that
1150 accounts for multiple levels of relatedness. Nat Genet 38:203–208. https://doi.org/10.1038/ng1702

1151 Yuan C, Singh RP, Liu D, et al (2020) Genome-Wide Mapping of Adult Plant Resistance to Leaf Rust
1152 and Stripe Rust in CIMMYT Wheat Line Arableu#1. Plant Dis 104:1455–1464.
1153 https://doi.org/10.1094/PDIS-10-19-2198-RE

1154 Yuan F-P, Zeng Q-D, Wu J-H, et al (2018) QTL Mapping and Validation of Adult Plant Resistance to
1155 Stripe Rust in Chinese Wheat Landrace Humai 15. Front Plant Sci 9:968.
1156 https://doi.org/10.3389/fpls.2018.00968

1157 Zelba O, Wilderspin S, Hubbard A, et al (2024) The adult plant resistance (APR) genes Yr18, Yr29 and
1158 Yr46 in spring wheat showed significant effect against important yellow rust races under North-

West European field conditions. Euphytica 220:1–15. https://doi.org/10.1007/s10681-024-03355-w

Zeng Q, Wu J, Liu S, et al (2019a) Genome-wide mapping for stripe rust resistance loci in common wheat cultivar Qinnong 142. Plant Dis 103:439–447. https://doi.org/10.1094/PDIS-05-18-0846-RE

Zeng Q, Wu J, Liu S, et al (2019b) A major QTL co-localized on chromosome 6BL and its epistatic interaction for enhanced wheat stripe rust resistance. Theoretical and Applied Genetics 132:1409–1424. https://doi.org/10.1007/s00122-019-03288-2

Zhang J, Gizaw SA, Bossolini E, et al (2018) Identification and validation of QTL for grain yield and plant water status under contrasting water treatments in fall-sown spring wheats. Theoretical and Applied Genetics 131:1741–1759. https://doi.org/10.1007/s00122-018-3111-9

Zhang P, Li X, Gebrewahid TW, et al (2019) QTL Mapping of Adult-Plant Resistance to Leaf and Stripe Rust in Wheat Cross SW 8588/Thatcher using the Wheat 55K SNP Array. Plant Dis 103:3041–3049. https://doi.org/10.1094/PDIS-02-19-0380-RE

Zhou X, Zhong X, Roter J, et al (2021) Genome-Wide Mapping of Loci for Adult-Plant Resistance to Stripe Rust in Durum Wheat Svevo Using the 90K SNP Array. Plant Dis 105:879–888. https://doi.org/10.1094/PDIS-09-20-1933-RE

Zhou XL, Han DJ, Chen XM, et al (2015) QTL mapping of adult-plant resistance to stripe rust in wheat line P9897. Euphytica 205:243–253. https://doi.org/10.1007/s10681-015-1447-7

Zhu C, Gore M, Buckler ES, Yu J (2008) Status and Prospects of Association Mapping in Plants. Plant Genome 1:5–20. https://doi.org/10.3835/plantgenome2008.02.0089

Zhu C, Yu J (2009) Nonmetric Multidimensional Scaling Corrects for Population Structure in Association Mapping With Different Sample Types. Genetics 182:875–888. https://doi.org/10.1534/genetics.108.098863

Zhu T, Wang L, Rimbert H, et al (2021) Optical maps refine the bread wheat Triticum aestivum cv. Chinese Spring genome assembly. Plant Journal 107:303–314. https://doi.org/10.1111/tpj.15289

Zuk O, Schaffner SF, Samocha K, et al (2014) Searching for missing heritability: Designing rare variant association studies. Proc Natl Acad Sci U S A 111:. https://doi.org/10.1073/pnas.1322563111

Statements & Declarations

Funding

This research was supported by the National Agency of Research and Innovation of Uruguay (ANII) through the INNOVAGRO program grant FSA_1_2018_1_152918 and POS_FSA_2019_2_1009141, the Sectoral Commission for Scientific Research of Uruguay (CSIC) through the research initiation program 22320200200059UD, and the Postgraduate Academic Commission (CAP) scholarship for completion of postgraduate studies.

Competing Interests

The authors declare that they have no conflict of interest.

Author Contributions

SG conceived and designed the study. SG and PS coordinated and planned the activities. VR prepared the manuscript. SG, PS, MK, BL, FC, AC, CP, and LG contributed with corrections and suggestions. VR performed the bioinformatics analysis with support from BL and LG. VR and RG conducted the field phenotyping. RG, FP, and NP supported field experiments. VR conducted greenhouse experiments and laboratory work. RG provided support for the greenhouse experiments. MQ provided some of the wheat lines included in the panel.

Acknowledgements

We would like to thank Inés Rebollo and Pablo Sandro for their contributions to the bioinformatics analyses, Wanda Iriarte from the biotechnology laboratory at INIA Las Brujas for her support with the genotyping of KASP markers, Martina Villero for her collaboration in the laboratory at INIA La Estanzuela, and María Flores and Kathy Díaz for maintaining the field trials.

Supplementary material

Tables

Table S1. Phenotypic data: adjusted means (BLUEs) of combined field data from both years (AUDPC) and seedling test (IT), days to heading, presence/absence information for the identified QTL and information on the allele (1, favorable YR resistant allele; 2, YR susceptible allele), number of favorable alleles per line, and presence/absence of *Yr18*, *Yr29* and *Yr46* genes by KASP markers. NA, missing information.

Table S2. Fit indicators of the area under the disease progress curve (AUDPC) data analysis models for the 366 wheat lines from 2021, 2022, and both years combined.

Table S3. Comparison of the physical position of the quantitative trait loci (QTL) identified as regions associated with resistance to yellow rust and genes and QTL, based on Tong e t al. (2024) previous review.

Figures

Figure S1. Scatter and frequency distributions and Pearson's correlation coefficients for yellow rust (YR) area under the disease progress curve (AUDPC) across 366 wheat lines in the panel evaluated under field conditions. Panels represent data for: A) 2021, B) 2022, and C) combined years (2021 and 2022). Histograms along the diagonal represent frequency distributions of YR AUDPC, while scatter plots of YR AUDPC among replicates are shown in the lower-left panels. Pearson's correlation coefficients for AUDPC between corresponding replicates (A&B) and years (C) are displayed in the upper-right panels. *** Significant correlations at $P < 0.001$.

Figure S2. Number of lines with different seedling yellow rust infection type (IT) for the *Triticale2015a* and *Triticale2015b* races.

Figure S3. Distribution of field yellow rust residuals' values according to the base and models with spatial column information for 2021 (A) and 2022 (B). Histograms of residuals according to the base model and models with spatial information for 2021 (C) and 2022 (D) for the variable area under the disease progress curve (AUDPC) of the 366 wheat lines.

Figure S4. SNP density plot showing the distribution of the 156,034 SNPs by wheat chromosome.

Figure S5. Heatmap of Euclidean distances where lines are ordered bases on cluster analysis among the 366 wheat lines of the GWAS and GP panel (A). Principal co-ordinate analysis (PCoA) for the 366 wheat lines of the GWAS and GP panel, colors indicate the AUDPC value for each line on a temperature scale from green (low) to red (high) (B). PCoA where colors indicate the origin of the lines (lines from National Institute of Agronomical Research (INIA) - Resistant Germplasm Development Program (INIA-RGDP); advanced, elite, and released lines of INIA - Wheat Breeding program (INIA-WBP); cultivars from other breeding programs that have been grown in Uruguay and checks) (C). Values of the delta k from Admixture (D).

Figure S6. Manhattan plots for yellow rust (YR) resistance based on infection type (IT) values for race *Triticale2015a* (A) *Triticale2015b* (B) and for days to heading (C) in 366 wheat lines of the panel. Horizontal line indicating the genome-wide significance threshold.

Figure S7. Predictive ability expressed as the Pearson's correlation between observed and predicted values (A), and mean squared error (MSE, B) of seven genomic prediction (GP) models for yellow rust (YR) resistance based on area under the disease progress curve (AUDPC) values in the field evaluations. Models compared include Pedigree-based (A-BLUP), G-BLUP, RR-BLUP, Bayesian A (BA), Bayesian

B (BB), Bayesian C (BC), and Bayesian LASSO (BL). Results are based on a 10-fold cross-validation scheme with 100 iterations. Boxplots show the distribution of a dataset through five key summary statistics: minimum (lower whisker), first quartile (bottom of the box), median (line inside the box), third quartile (top of the box), and maximum (upper whisker). Points beyond the whiskers are values outside 1.5 times the interquartile range from the quartiles.

Figure S8. Predictive ability expressed as the Pearson's correlation between observed and predicted values (A), and mean squared error (MSE, B) of the G-BLUP model prediction for yellow rust (YR) resistance based on area under the disease progress curve (AUDPC) values in the field evaluations incorporating QTL as fixed effects. The model progressively incorporates up to five QTL identified via genome-wide association study (GWAS) as fixed effects. Results are based on a 10-fold cross-validation scheme with 100 iterations. Boxplots show the distribution of a dataset through five key summary statistics: minimum (lower whisker), first quartile (bottom of the box), median (line inside the box), third quartile (top of the box), and maximum (upper whisker). Points beyond the whiskers are values outside 1.5 times the interquartile range from the quartiles.

Figure S9. Quantile–quantile (QQ) plots of observed vs. expected p-values, obtained from the GWAS model used to detect QTL for the variables (A) field AUDPC, (B) seedling IT for the *Triticale2015a* race, (C) seedling IT for the *Triticale2015b* race.

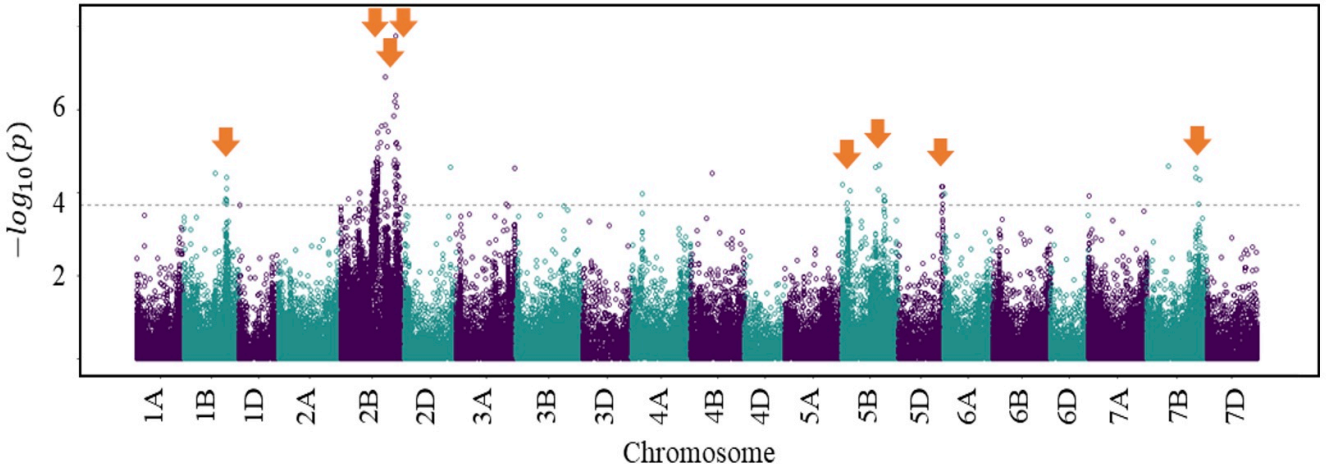
$-log_{10}(p)$
6
4
2
1A
1B
1D
2A
2B
2D
3A
3B
3D
4A
4B
4D
5A
5B
5D
6A
6B
6D
7A
7B
7D
Chromosome

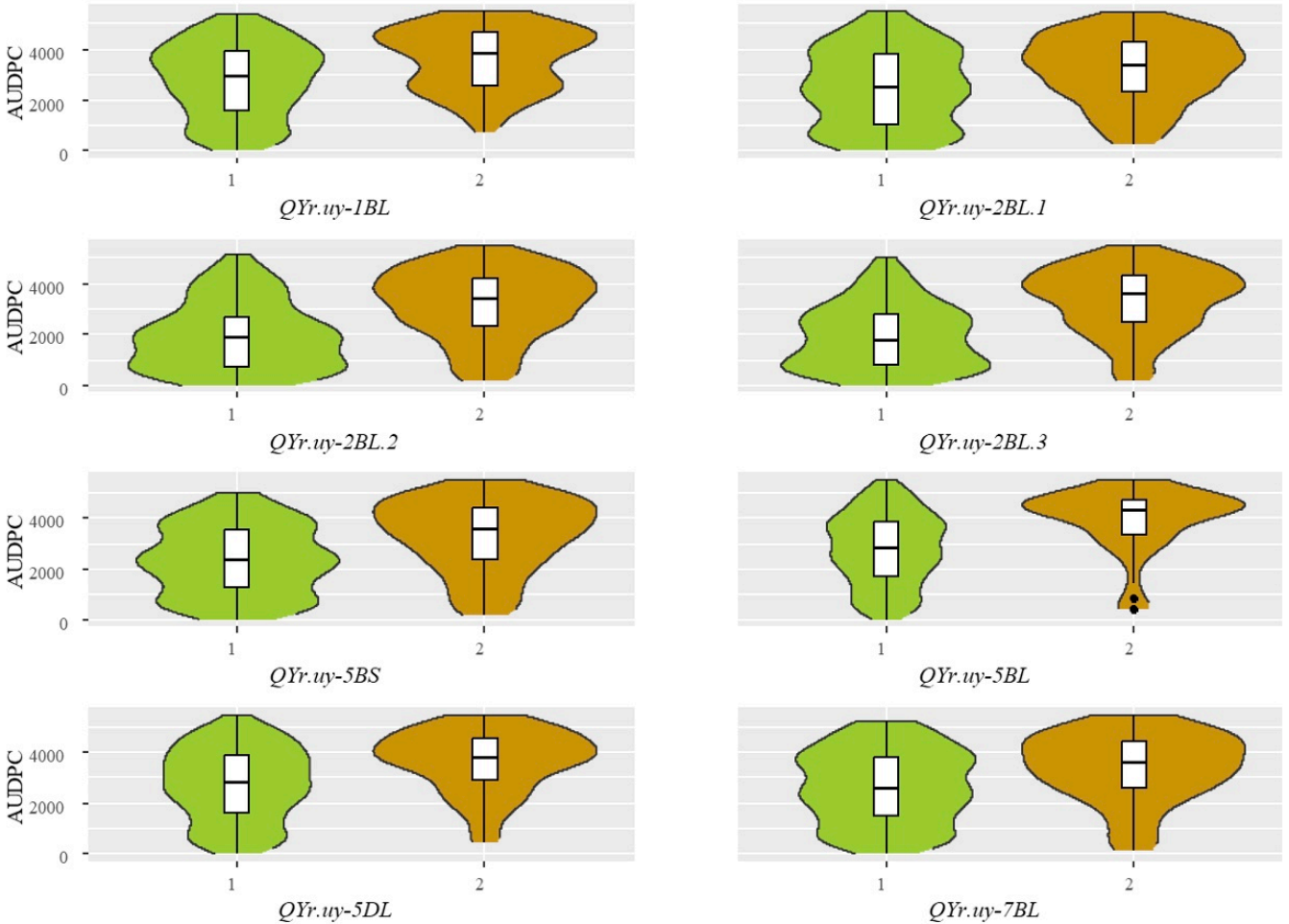
AUDPC
4000
2000
0
1
2
QYr.uy-1BL
QYr.uy-2BL.1
QYr.uy-2BL.2
QYr.uy-2BL.3
QYr.uy-5BS
QYr.uy-5BL
QYr.uy-5DL
QYr.uy-7BL

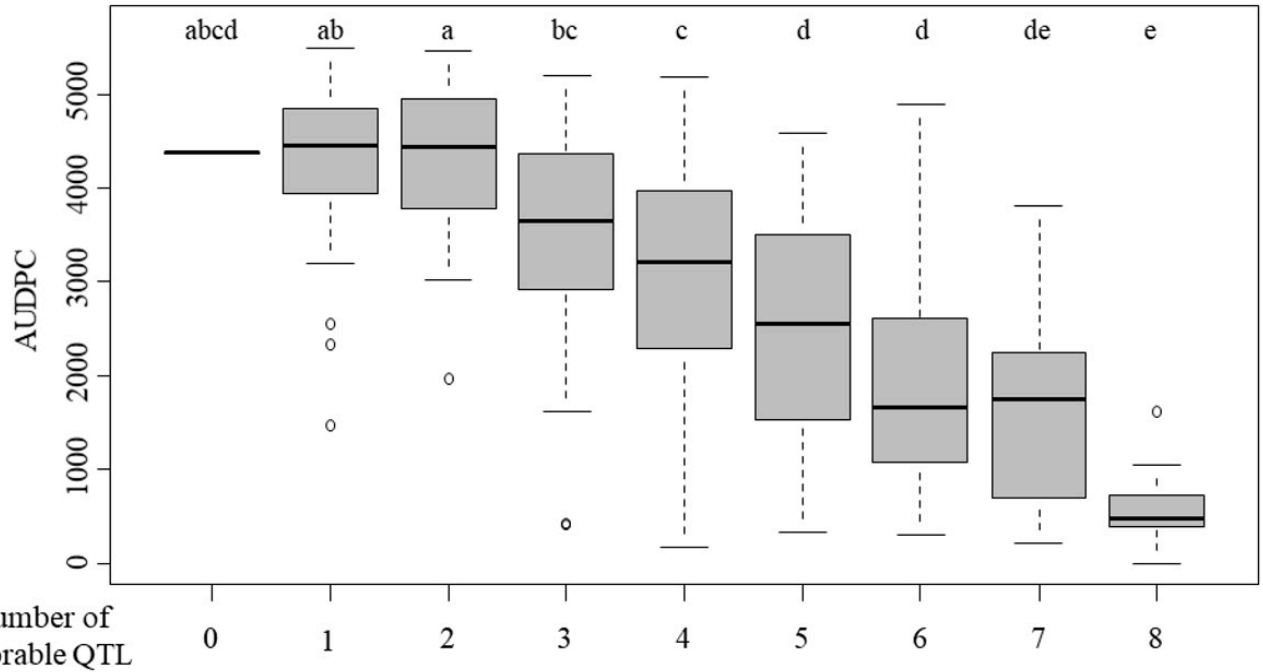

	Number of lines in each group								
INIA-RGDP	0	7	16	24	54	41	14	13	3
INIA-WBP	0	5	16	24	39	21	5	5	2
Other breeding programs	1	6	9	9	11	11	10	10	6
Total	1	18	41	57	104	73	29	28	11